LA-UR-01-6804
Approved for public release;
distribution is unlimited.

Title: **User Manual for the Code LAQGSM**

Author(s): Konstantin K. Gudima, Stepan G. Mashnik, and Arnold J. Sierk

Submitted to:

http://lib-www.lanl.gov/la-pubs/00818645.pdf

User Manual for the Code LAQGSM

Konstantin K. Gudima[1,2], Stepan G. Mashnik[1], and Arnold J. Sierk[1]

[1]*Nuclear Physics Group, T-16*
Theoretical Division, MS B283
Los Alamos National Laboratory
Los Alamos, NM 87545, USA
(E-mail: mashnik@t2y.lanl.gov)
(E-mail: ajs@t2ajs.lanl.gov)

[2]*Institute of Applied Physics*
Academy of Sciences of Moldova
Kishinev, MD-2028, Moldova
(E-mail: gudima@cc.asm.md)

Abstract

The Los Alamos version of the Quark-Gluon String Model (LAQGSM) is implemented in a universal Monte-Carlo code, LAQGSM, for simulating hadron-nucleus and nucleus-nucleus reactions at energies from $\sim$ 20 MeV up to $\sim$ 200 GeV per nucleon. The following physics models are implemented in LAQGSM to simulate the different physics processes involved in various reactions to be calculated by the code: the Dubna intranuclear Cascade Model (DCM), the Quark-Gluon String Model (QGSM), an improved version of the Cascade-Exciton Model (CEM) contained in the code CEM2k, the Fermi break-up model, and the coalescence model. This Manual briefly describes the main assumptions of the models incorporated into LAQGSM, gives essential technical details of the code such as a description of the main parameters, presents a complete description of the input and output files, and provides readers with necessary information for a practical use of the code.

Los Alamos, December, 2001

Contents

1. Introduction

A large amount of reliable nuclear reaction data on proton- and nucleus-nucleus interactions at incident energies from tens to hundreds of GeV/nucleon is required for different applications, *e.g.*, for the recent project on Proton Radiography for an Advanced Hydrotest Facility [1], to examine the radiation environment at high energy accelerators such as the Relativistic Heavy-Ion Collider (RHIC) at Brookhaven, the Large Hadron Collider (LHC) and the Super Proton Synchrotron (SPS) at CERN, to solve astrophysical problems, *etc.* Experiments to measure these data are costly and there are a limited number of facilities available to make such measurements. Therefore reliable models are required to provide the necessary data.

On the other hand, for solving different purely academic problems, such as studying strongly interacting matter at high density and/or temperature and to investigate the Quark-Gluon Plasma, one needs again reliable models and codes. One such model may be the Los Alamos version of the Quark-Gluon String Model as implemented in the code LAQGSM. LAQGSM is a product of many years of work by several groups of nuclear theorists and code developers and is a system combining the Dubna intranuclear Cascade Model (DCM) [2]–[6], the Quark-Gluon String Model (QGSM) [7]–[12], the improved version of the Cascade-Exciton Model (CEM) [13] implemented in the code CEM2k [14]–[17], the Fermi break-up model [18], and the coalescence model presented in Refs. [5, 19].

In the next section we briefly describe all models used in LAQGSM. Then in Sec. 3 we describe the main parameters of the code that are fixed but may be changed in some cases by users to study specific physical effects. We give also details about all physical characteristics of a simulated reaction stored in common blocks of LAQGSM, so that users may modify the output of the code by writing their own routines to get a needed output for each concrete application of LAQGSM. In sections 4 and 5, we present a description of all input and output parameters of the code (an example of input and output files is given in the Appendix). Sec. 6 is devoted to acknowledgments, followed by References and an Appendix.

2. Basic assumptions of LAQGSM

2.1. Dubna intranuclear Cascade Model (DCM)

The core of the LAQGSM is built on a version of the intranuclear cascade model developed at Dubna [2]–[6], often referred in the literature simply as the **D**ubna intranuclear **C**ascade **M**odel (DCM). A detailed description of the DCM may be found in Refs. [2]–[6], so only its basic assumptions will be outlined here. DCM is a universal intranuclear cascade model to describe both hadron- and nucleus-nucleus interactions. Historically, it was developed [2, 3, 4, 5] to describe nucleus-nucleus interactions at incident energies up to several GeV/nucleon, without any connection to the Quark-Gluon String Model. That version of the DCM is similar to other intranuclear cascade models for heavy-ion reactions, such as the model by Yariv and Fraenkel (the code ISABEL [20, 21]) and the Liège code by Cugnon *et al.* [22], all reviewed in Fraenkel [23].

In contrast to the earlier versions of the intranuclear cascade model developed at Dubna, this version of DCM uses a continuous nuclear density distribution (instead of the approximation of several concentric zones, where inside each the nuclear density is considered to

be constant; therefore, it does not need to consider refraction and reflection of cascade particles inside or on the border of a nucleus); it also keeps track of the time of intranuclear collisions and of the depletion of the nuclear density during the development of the cascade (the so-called "trawling effect").

The DCM models interactions of fast cascade particles ("participants") with nucleon spectators of both the target and projectile nuclei and includes as well interactions of two participants (cascade particles). It uses experimental cross sections (or those calculated by the Quark-Gluon String Model for energies above 4.5 Gev/nucleon) for these elementary interactions to simulate angular and energy distributions of cascade particles, also considering the Pauli exclusion principle. Mathematically, an intranuclear cascade is described by a modified relativistic Boltzmann equation for a mixture of gases of stable hadrons and short-lived resonances

$$p^\mu \partial_\mu f_i(x,p) = \sum_j C_{coll}(f_i, f_j) + \sum_k R_{k\to i}(f_k), \tag{1}$$

where $f_i(x,p)$ is a one-particle distribution function for the hadrons of type i. The first term in the right-hand side of this equation accounts for two- body collisions and the second term describes the resonances decaying into particles of type i with 4-momentum $p = (E, \vec{p})$ and 4-coordinate $x = (t, \vec{x})$. It is convenient to consider separately equations for the spectator nucleons of the target (index T) and projectile nucleus (index P) and for participating hadrons (*i.e.*, "cascade particles") including both stable hadrons (index S) and resonances (index R). Then the system of equations assumes the following form [10, 11]: for spectator nucleons of the target,

$$p^\mu \partial_\mu f_T(x,p) = -f_T(x,p) \left[\sum_{j=R,S,P} \int d\omega_j f_j(x,p_j) Q_{Tj} \sigma^{Tj} \right]; \tag{2}$$

for spectator nucleons of the projectile nucleus it is necessary in Eq. (2) to make the substitution of indices $P \to T$ and $T \to P$; for stable hadron participants,

$$\begin{aligned} p^\mu \partial_\mu f_S(x,p) &= \\ &- f_S(x,p) \left[\sum_{j=T,P,R,S'} \int d\omega_j f_j(x,p_j) Q_{Sj} \sigma^{Sj} \right] + \\ &+ \int d\omega_P d\omega_T \Phi(p_P, p_T | x, p, \tau_f) + \\ &+ \sum_{j=T,P} \sum_{k=R,S'} \int d\omega_j d\omega_k \Phi(p_j, p_k | x, p, \tau_f) + \\ &+ \sum_{j=R',S''} \sum_{k=R,S'} \int d\omega_j d\omega_k \Phi(p_j, p_k | x, p, \tau_f) + \\ &+ \sum_R \int d\omega_{S'} d\omega_R f_R(x,p_R) \Gamma^{R\to S+S'} \delta^{(4)}(p_R - p_{S'} - p), \end{aligned} \tag{3}$$

and a similar equation for hadronic participant resonances. Here, the quantity $Q_{ij} = [(p_i p_j)^2 - p_i^2 p_j^2]^{1/2}$ is related to the relative velocity of the colliding hadrons $|\vec{v}_i - \vec{v}_j| = Q_{ij}/E_i E_j$ and $d\omega = d^3p/E$ is the invariant volume element in momentum space. The rate of hadron

formation Φ entering into Eq. (3) can be expressed in terms of the probability of collision (per unit time) between hadrons i and j, $\simeq f_i f_j Q_{ij} \sigma^{ij}$, as follows:

$$\Phi(p_i, p_j | x, p, \tau_f) = \int dx' f_i(x', p_i) f_j(x', p_j) Q_{ij} \sigma^{ij} \phi(x' | x, p, \tau_f), \tag{4}$$

where $\phi(x'|x, p, \tau_f)$ is the transition probability of detecting a hadron at the point x if the collision took place at the space-time point x' [10, 11].

In the initial version of the DCM [2]–[5], only Δ resonances were taken into account, no interactions between two cascade particles (participants) were considered, and no formation time, τ_f, for participants was used in calculations. All elementary cross sections were taken from available experimental data. Cascade particles are traced until their energy decreases due to elementary collisions to a value equal or below the cutoff energy of 1 MeV (plus the Coulomb barrier, for protons) above the Fermi level, when they are considered to be absorbed by the target/bombarding nucleus, increasing its excitation energy. When all of the cascade particles escape from or are absorbed by the target and bombarding nuclei, the reaction is considered to pass to the preequilibrium stage [13], followed by the final evaporative stage. If the excited residual nuclei remaining after the cascade stage of a reaction from the target and bombarding nuclei have mass numbers lower than $A \leq 13$, the Fermi break-up model [18] is used by DCM after the cascade stage of the interaction instead of using the preequilibrium and evaporation stages. The low-energy, initial version of the DCM [2]–[5] is used in LAQGSM for nucleon-, pion-, and nucleus-nucleus interactions at incident energies up to 4.5 GeV/nucleon. To make the DCM code applicable at higher energies (up to about 200 GeV/nucleon), it was merged with the Quark-Gluon String Model (QGSM) [7]–[12] described briefly in the next subsection.

2.2. Quark-Gluon String Model (QGSM)

In a nuclear reaction at ultrarelativistic energies, both the initial and the final states are hadronic states. However, in the intermediate state, the quark-gluon degrees of freedom are unfrozen, and we are dealing with a certain displaced quark-hadron state, including even the possible formation of a quark-gluon plasma [11]. The fundamental theory must describe both the evolution of the hadronic and quark phase and the processes of deconfinement and hadronization. Since the complete solution of this program is beyond the possibility of modern theory, the Quark-Gluon String Model (QGSM) describes nuclear collisions in the approximation of independent quark-gluon strings [8]–[12]. In the quasiclassical treatment, collisions of quark-gluon strings lead to the formation of bends of the strings, *i.e.*, kinks. In the QGSM, the leading edges of bent strings are replaced by energetic hadrons; this corresponds to minimal inclusion of quark dynamics [8]–[12]. This means that the basic kinetic equations will be written in terms of hadronic states, *i.e.*, we may use once again Eqs. (1–4). However, the quark properties are used for specifying the initial hadron-hadron states (quark-gluon string model) and for describing the passage of strings through nuclear matter (introducing the concept of hadron formation time).

Mathematically, the function ϕ in Eq. (4) describes the evolution of the quark-gluon system or of a string-type object formed as a result of the collision, including the process of subsequent hadronization of the system with the hadrons on the mass shell. The set of parameters characterizing this evolution is denoted by τ_f [10, 11]. In general, the function ϕ must be obtained by solving an evolution equation allowing for the influence of the nuclear

environment and for the possibility of interaction between the strings formed. QGSM [10, 11] uses the simplest case in which the approximation of a finite time of hadron formation is used for the transition probability:

$$\phi(x'|x,p,\tau_f) = \frac{1}{\sigma}\frac{d\sigma}{d\omega}\delta(t-t'-\tau_f)\delta^{(3)}\left(\vec{x}-\vec{x}'-\frac{\vec{p}}{E}(t-t')\right)F(\tau_f). \tag{5}$$

In other words, QGSM [10, 11] assumes that a hadron with spectral distribution $(1/\sigma)(d\sigma/d\omega)$ is "prepared" at the collision point x', then moves freely up to the point x, but becomes observable (*i.e.*, is in the on-mass-shell state) only after passage of a time τ_f, generally distributed in accordance with some law $F(\tau_f)$. In the QGSM, we set $F(\tau_f) = 1$. During the formation time τ_f, the "prepared" hadron does not interact with the surrounding matter. For a hadron of mass m, τ_f can be related to the proper time of hadron formation τ_f^0 as $\tau_f = (E/m)\tau_f^0$, and τ_f^0 can be fixed from an analysis of experimental data on hadron-nucleus interactions. To find the spectral distributions $(1/\sigma)(d\sigma/d\omega)$ of particles produced in relativistic hadron-hadron collisions, QGSM uses the model of quark-gluon strings. In the limit $\tau_f^0 \to 0$, the equations (2) and (3) reduce to the ordinary relativistic Boltzmann equations [10, 11].

QGSM assumes that the main contribution to hadron production is due to soft interaction processes. To describe them, QGSM uses the Dual Parton Model (DPM) [24] and its interpretation in terms of quark-gluon strings [25]. This model is based on the $1/N$ expansion of the amplitude of binary processes, where N is the number of colors or flavors. QGSM takes into account [10, 11] planar and cylindrical diagrams, as well as the so-called diagrams of an "undeveloped" cylinder, which are important at not very high, preasymptotic energies [26]. All the included processes in the case of the πN interaction are shown in Fig. 1, adapted from [11].

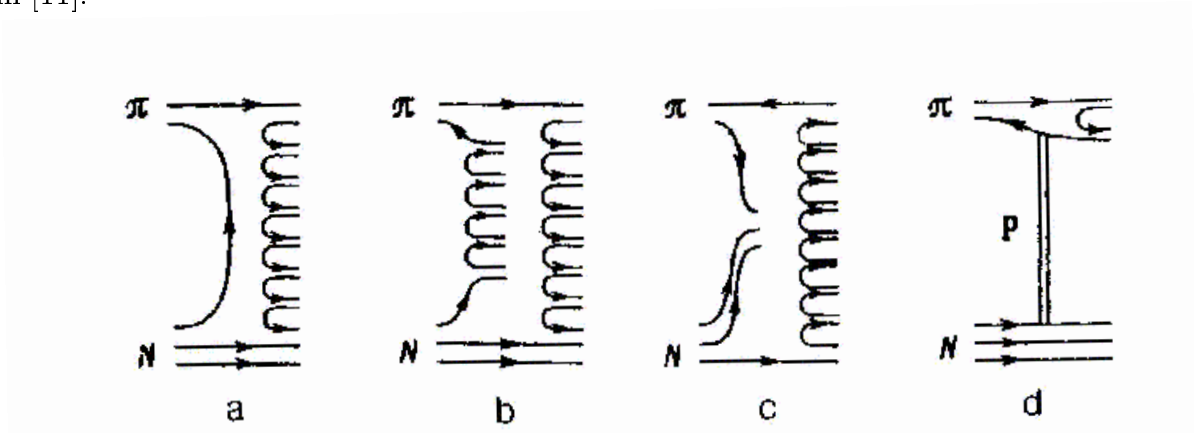

Figure 1: Topological diagrams of the processes of multiple production of particles in πN collisions, including in the model the processes: a—planar; b—cylindrical; c—undeveloped cylinder; d—diffractive (adapted from Ref. [11]).

The partial cross section for this interaction are given by the expression

$$\sigma_{tot} = \sigma_{pl} + \sigma_{cyl} + \sigma_{und} + \sigma_{dif} + \sigma_{el}. \tag{6}$$

Here the cross section

$$\sigma_{pl} = 8\pi\gamma_R(s/s_0)^{\alpha_R(0)-1} \tag{7}$$

corresponds to the process, described by the planar diagram in Fig. 1a, which involves annihilation of a quark and an antiquark and formation of one quark-gluon string. In Eq. (7), the Reggeon residue and intercept are, respectively, $\gamma_R = 0.663$ GeV^{-2} and $\alpha_R = 0.5$ [10, 11]. The cross section for the "undeveloped" cylindrical diagram of Fig. 1c is given by the following expression [26]:

$$\sigma_{und} = 24\pi\gamma_R\sqrt{\gamma_P/4\lambda_R}(s/s_0)^{\alpha_R(0)-1}(s/s_0)^{\Delta/2}, \tag{8}$$

where the Pomeron residue is $\gamma_P = 3$ GeV^{-2}, and $\Delta \equiv \alpha_p - 1 = 0.1$. The parameter λ_R characterizes the dependence of the amplitude of Reggeon exchange on the momentum transfer,

$$\lambda_R = R^2 + \alpha'_R \ln(s/s_0). \tag{9}$$

For the remaining parameters, the following values were taken [11]: $\alpha'_R = 0.25$ GeV^{-2}, $R^2 = 1.695$ GeV^{-2}, and $s_0 = 2$ GeV^2.

In the case of diffractive production of hadrons (Fig. 1d), QGSM assumes that $\sigma_{dif} = 0.5\sigma_{el}$. The main contribution to the process of hadron production at high energies is due to the cylindrical diagram corresponding to exchange of color between the colliding particles, with subsequent formation of two strings. The cross section for this process is found from Eq. (6), in which the experimental values of σ_{tot} and σ_{el} are used. The formation and decay of quark-gluon strings is modeled by the Monte-Carlo method. The mass and momentum of a string are determined by the quark content of the string and by the momentum distribution of the constituent quarks. The asymptotics of these functions for $x \to 0$ and $x \to 1$ follows from a Reggeon analysis of the planar diagrams [26]. In particular, for the processes shown in Figs. 1b and 1c, QGSM uses the following distributions in the fraction x of the momentum carried by the quarks in a baryon (B) and a meson (M):

$$u_B(x) \sim x^{-1/2}(1-x)^a, \tag{10}$$

$$u_M(x) \sim x^{-1/2}(1-x)^{-0.5}, \tag{11}$$

where the exponents are $a = 1.5$ and 2.5, respectively, for the u and d quarks in a proton, and vice versa in the case of a neutron. The transverse momentum distribution of the constituent quarks is given by

$$\omega(p_\perp) = (\pi\sigma_\perp^2)^{-1/2}\exp(-p_\perp^2/\sigma_\perp^2) \tag{12}$$

with an average transverse momentum $\sigma_\perp = 0.51$ GeV/c, as used in the present version of LAQGSM.

In the case of diffractive dissociation, the transverse momentum of a quark in an excited hadron is determined by the sum of two terms: the transverse component of the recoil momentum of the unexcited hadron and the transverse momentum of the constituent quarks. Both quantities are described by the distribution (12), but a smaller value of the parameter $\sigma_\perp = 0.25$ GeV/c is used for the recoil momentum. As for the x distribution of quarks in diffraction processes, Eq. (10) is used for it once again, with the quarks assumed to be massless. With this choice of parameters, the position of the maximum in the distribution in the diffraction mass M_{dif} in the region of the resonance $N^*(1470)$ is satisfactorily described for diffractive production in hadron-hadron collisions, and so is the behavior at higher values of M_{dif}, where the distribution falls off faster than $1/M_{dif}^2$ (see [27, 28]).

The processes of fragmentation of quarks, antiquarks, and diquarks are modeled in QGSM by the Field-Feynman method [29]. The fragmentation functions are chosen in the form

$$\begin{aligned} f_{q\to M}(z) &= 1-a+2a(1-z), \\ f_{qq\to B}(z) &= 0.4+0.6\exp[-20(1-z)]/[1+\exp(-20)], \\ f_{qq\to M}(z) &= 3a(1-z)^2, \end{aligned} \tag{13}$$

where $a = 0.7$ and $z = (E_q + p_{\|})/W_q$ is the light-cone variable for a quark belonging to a created hadron. It is assumed that the total transverse momentum of a quark-antiquark pair produced by the rupture of a string is zero, and the momenta of the individual quarks of this pair are given by the distribution

$$\omega(p)^2_{\perp})d^2p_{\perp} = Ad^2p_{\perp}/(1+bp^2_{\perp})^4 \sim \exp(-3bp^2_{\perp})d^2p_{\perp} \tag{14}$$

with the parameter $b = 1.3$ Gev$^{-2}\cdot$ sec^2.

QGSM includes the u, d, and s quarks. Vacuum pairs are generated with relative probabilities $P_{u\bar{u}} : P_{d\bar{d}} : P_{s\bar{s}} = 1 : 1 : 0.30$. The ratio 3 : 1 was taken as the relative probability of formation of vector and pseudoscalar mesons. Mixing of the neutral mesons π^0, ρ^0, ω^0, η^0, and η'^0 is taken into account in QGSM [11]. This version of the QGSM describes adequately the global characteristics of hadron-hadron collisions at energies above about 10 GeV/nucleon [27, 28].

To extend the applicability of the model to lower energies, QGSM was developed further in Ref. [12], where a phenomenological approximation for the characteristics of the hadron interactions was introduced at energies ≤ 10 GeV. In addition, in Ref. [12] a number of previously neglected phenomena like production of antibaryons with a possiblity of their subsequent interaction, taking into account participant-participant collisions, including meson-meson interactions, and other refinements were incorporated into the model.

For instance, in contrast to Refs. [8]–[11], where the probability of collision of the hadrons i and j was found allowing for transparency (an option commented out, but available in the code LAQGSM), the approximation of a "black disc" was used in Ref. [12] :

$$P(b^2_{ij}, s) = \theta(b^2_{ij} - \sigma(s)/\pi). \tag{15}$$

The two methods lead to practically identical results, but the latter method requires significantly less computer time, and is incorporated into LAQGSM as a default option. In expression (15), b_{ij} is the distance of minimum approach of the particles determined in the rest frame of one of the colliding partners. This quantity can be written in the frame of the observer as

$$\begin{aligned} b^2_{ij} &= (\vec{r}_i - \vec{r}_j)^2 + \left[\frac{\vec{p}_i(\vec{r}_i - \vec{r}_j)}{m_i}\right]^2 - \\ &- \left[\frac{\vec{p}_j(\vec{r}_i - \vec{r}_j)/E^*_j - \vec{p}_i(\vec{r}_i - \vec{r}_j)/m_i}{1-(m_j/E^*_j)^2}\right], \end{aligned} \tag{16}$$

where particle i is characterized by the coordinate $\vec{r}_i$, the momentum $\vec{p}_i$, and the mass m_i, and E^*_j is the energy of particle j in the rest frame of particle i.

In the determination of the probability of interaction of the produced hadrons, QGSM uses the experimentally measured cross sections $\sigma(s)$. In those cases when such data do not

exist, QGSM uses the relations following from isotopic invariance of the strong interactions in the additive quark model (for example, for finding the cross sections for meson-meson interactions). The cross sections for the interaction of resonances are assumed to be equal to the cross sections for the interaction of the stable particles with the same quark content. The cross section for the interaction of strange baryons and nucleons are poorly known. However, at an initial energy around 20 GeV the cross-section ratio $\sigma(\Sigma^- p)/\sigma(pp)$ or $\sigma(\Lambda p)/\sigma(pp)$ is approximately 0.82, in agreement with the quark model (see details in [12]). Therefore, if a hadron consists of n_s strange quarks, its cross section is smaller by a factor of $(0.82)^{n_s}$ than the cross section for the interaction of a non-strange hadron. For example, the cross section $\sigma(KK)$ can be expressed in terms of the experimentally measured cross section $\sigma_{exp}(KN)$ as follows: $\sigma(KK) = 0.82(2/3)\sigma_{exp}(KN)$ [12].

The lifetimes of the resonance particles are determined in QGSM by an exponential distribution with a slope expressed in terms of the tabulated decay width, provided in the code LAQGSM by the routine ATAB.DAT.

We return now to the parameters entering Eqs. (3)–(5): the formation time τ_f^0. Strictly speaking, the concept of formation time is clearly defined only for the formation of structureless particles. In the case of a point hadron, the uncertainty principle gives a natural scale for the time-delay effect [8, 11]

$$\tau_f^0 \sim \hbar/m_\perp \tag{17}$$

and, correspondingly, for the length of hadron formation,

$$l_f = \tau_f^0 \gamma v \approx p/m_\perp^2. \tag{18}$$

In parton models of the hadron-nucleus interaction at high energies agreement with experiment can be achieved for transfer mass values $m_\perp \approx 0.5$ GeV, *i.e.*, the fast hadrons are mainly formed outside the nucleus. However, for a hadron treated as a constituent particle, the very concept of formation time becomes somewhat indeterminant, since the different constituents of a hadron can be formed at different times. Generally, different models predict different values for τ_f^0, but the length of formation of a fast hadron can be appreciably smaller than the estimate (18) (see details and references in [8, 11]).

Since the formation time is an open question and is model-dependent, QGSM considers τ_f^0 as free parameters fitted from the best description of available experimental data for proton-nucleus collisions at 200 GeV. Note that QGSM singles out the baryon formation time τ_B^0 having in mind that any baryon belongs always to the leading particles and, therefore is expected to be formed earlier in time [8, 11]. For all other stable hadrons and resonances the appropriate formation times are taken to be equal each to other and this quantity is denoted as τ_M^0. An analysis of hadron-nucleus reactions [8, 11] showed that in any version of QGSM it should be assumed that $\tau_B^0 \ll \tau_M^0$ to get a reasonable agreement with experimental data. Naturally, the limit $\tau_f^0 \to \infty$ would require that all produced particles pass through the nucleus without interactions, while the opposite limit (*i.e.*, $\tau_f^0 \to 0$) corresponds to a complete cascading with instantaneous formation of all hadrons.

The present version of the code LAQGSM uses as a default $t_f^0 = C_\tau \hbar/m_\pi$ in units of fm/c, with $C_\tau = 1.0$ for mesons and $C_\tau = 0$, for baryons. To get an idea on how the formation times used in LAQGSM affect the results of calculations, we show in Figs. 2 and 3 an example of spectra of nucleons, deuterons, antiprotons, pions and kaons emitted from the reaction p(70 GeV) + Al

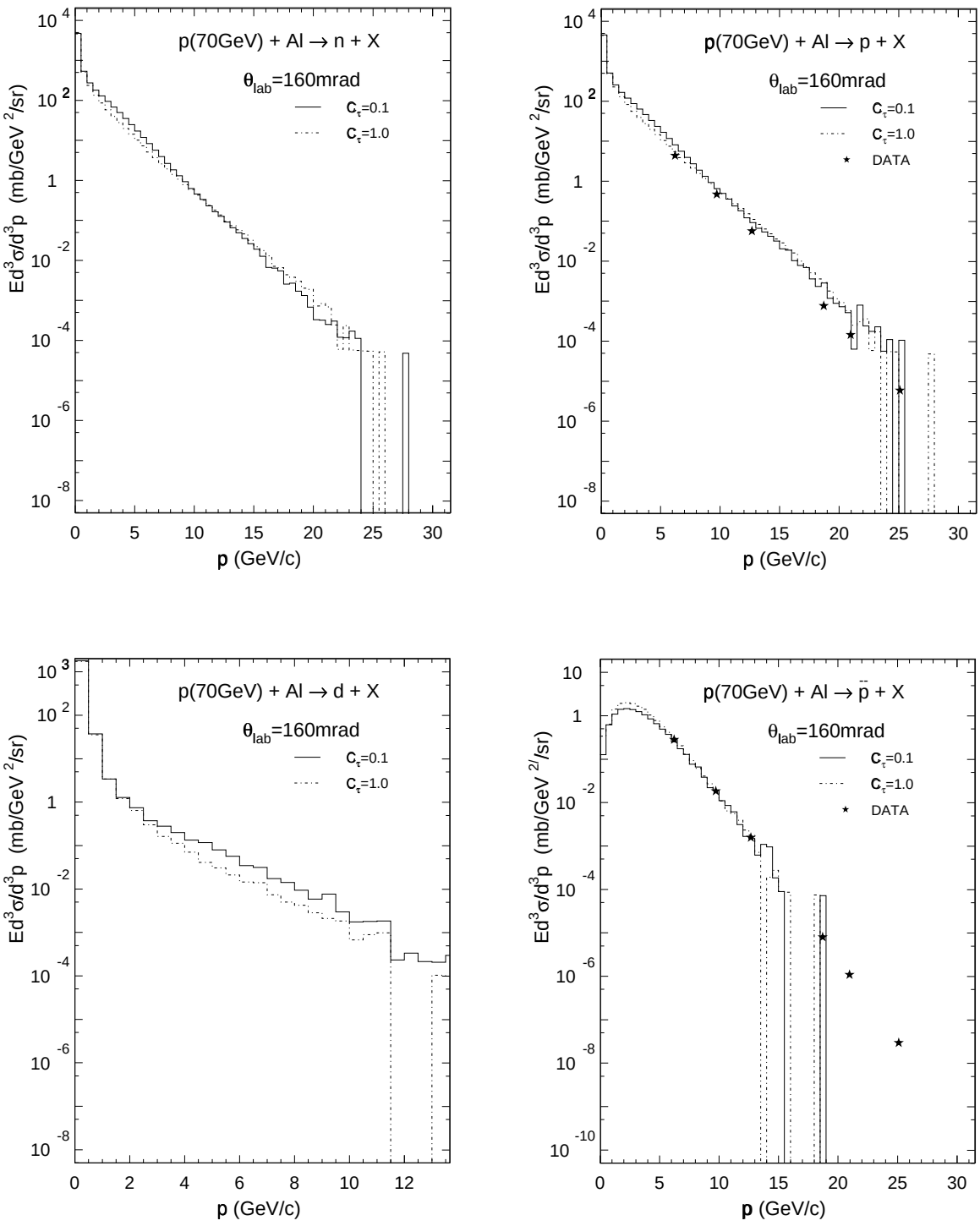

Figure 2: Invariant cross sections $Ed^3\sigma/d^3p$ for production of n, p, d, and $\bar{\text{p}}$ at 160 mrad from p+Al collisions at 70 GeV as functions of particle momentum p calculated with LAQGSM using $C_\tau = 0.1$ (solid histograms) and $C_\tau = 1.0$ (dashed histograms) compared with experimental data from [34].

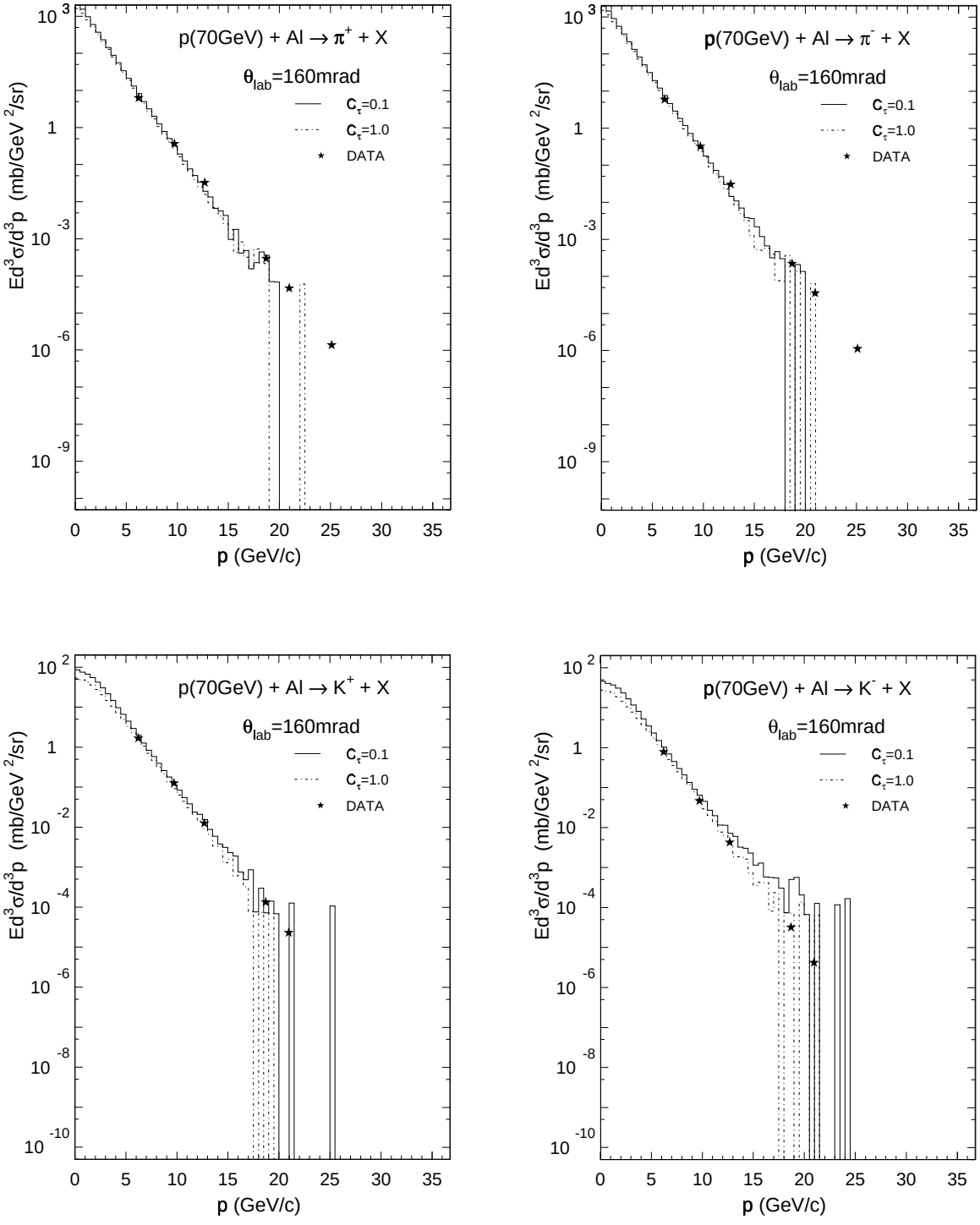

Figure 3: The same as Fig. 2, but for production of π^+, π^-, K^+, and K^-.

calculated by LAQGSM using $C_\tau = 1.0$ and $C_\tau = 0.1$ compared with experimental data [34].

Table 1 shows a comparison of the mean multiplicities of emitted particles calculated by LAQGSM with $C_\tau = 1.0$ and $C_\tau = 0.1$.

Table 1: Mean multiplicities of n, p, π^-, π^+, d, t, ^{3}He, ^{4}He, K^+, K^-, and $\bar{p}$ produced in p(70 GeV) + Al calculated by LAQGSM using $C_\tau = 0.1$ and $C_\tau = 1.0$

	n	p	π^-	π^+	d	t	^{3}He	^{4}He	K^+	K^-	$\bar{p}$
$C_\tau = 0.1$	5.17	5.17	3.95	4.27	0.877	0.223	0.158	0.860	0.338	0.176	0.017
$C_\tau = 1.0$	4.73	4.75	3.32	3.63	0.835	0.208	0.149	0.902	0.256	0.129	0.023

One can see that using a shorter formation time for mesons ($C_\tau = 0.1$) leads indeed to a more developed cascading and as a result, to a higher multiplicity for almost all secondary particles, except for ^{4}He and $\bar{p}$, in our example. Spectra of p, π^-, π^+, and K^+ calculated with $C_\tau = 0.1$ agree a little better with the data; spectra of $\bar{p}$ calculated with either value of C_τ are about the same; while the spectrum of K^- calculated with $C_\tau = 0.1$ tends to overestimate the data and agrees somewhat worse with the measurement than the one calculated using $C_\tau = 1.0$. Note that while the results of the two calculations shown above differ only slightly, the calculation using $C_\tau = 0.1$ requires about five time more computing time compared with the case of $C_\tau = 1.0$; therefore, we use in LAQGSM $C_\tau = 1.0$ by default.

2.3. Coalescence model

When the cascade stage of a reaction is completed, LAQGSM uses the coalescence model described in Refs. [5, 19] to "create" high-energy d, t, ^{3}He, and ^{4}He by final state interactions among emitted cascade nucleons, already outside of the target and projectile nuclei. In contrast to most other coalescence models for heavy-ion induced reactions, where complex particle spectra are estimated simply by convolving the measured or calculated inclusive spectra of nucleons with corresponding fitted coefficients (see, *e.g.*, [35] and references therein), LAQGSM uses in its simulation of particle coalescence real information about all emitted cascade nucleons and does not use integrated spectra. LAQGSM assumes that all the cascade nucleons having differences in their momenta smaller than p_c and a correct isotopic content form an appropriate composite particle. This means that the formation probability for, *e.g.*, a deuteron is

$$W_d(\vec{p},t,b) = \int\int d\vec{p}_p d\vec{p}_n \rho^C(\vec{p}_p,t,b)\rho^C(\vec{p}_n,t,b)\delta(\vec{p}_p+\vec{p}_n-\vec{p})\Theta(p_c-|\vec{p}^{\,c.m.}-\vec{n}^{c.m.}|), \quad (19)$$

where the particle density in momentum space is related to the one-particle distribution function f by

$$\rho^C(\vec{p},t,b) = \int d\vec{r} f^C(\vec{r},\vec{p},t,b). \quad (20)$$

Here, b is the impact parameter for the two interacting nuclei and the superscript index C shows that only cascade nucleons are taken into account for the coalescence process. The

coalescence radii p_c were fitted for each composite particle in Ref. [5] to describe available data for the reaction Ne+U at 1.04 GeV/nucleon, but the fitted values turned out to be quite universal and were subsequently found to satisfactorily describe high-energy complex particle production for a variety of reactions induced both by protons and nuclei at incident energies up to about 200 GeV/nucleon. These parameters used in the present version of LAGQSM are:

$$p_c(\mathrm{d}) = 90 \text{ MeV/c}; \qquad p_c(\mathrm{t}) = p_c(^3\mathrm{He}) = 108 \text{ MeV/c}; \qquad p_c(^4\mathrm{He}) = 115 \text{ MeV/c} . \tag{21}$$

If several cascade nucleons are chosen to coalescence into composite particles, they are removed from the status of nucleons and do not contribute further to such nucleon characteristics as spectra, multiplicities, *etc.*

2.4. Fermi break-up model

After calculating the coalescence stage of a reaction, LAQGSM moves to the description of the last slow stages of the interaction, namely to preequilibrium decay and evaporation, with a possible competition of fission. But as mentioned above, if the residual nuclei have atomic numbers with $A \leq 13$, LAQGSM uses the Fermi break-up model [18] to calculate their further disintegration instead of using the preequilibrium and evaporation models.

All formulas and details of the algorithms used in the version of the Fermi break-up model developed in the group of Prof. Barashenkov at the Joint Institute for Nuclear Research (JINR), Dubna, Russia and released in LAQGSM may be found in [36]. All the information needed to calculate a break-up of an excited nucleus is its excitation energy U and the mass and charge numbers A and Z. The total energy of the nucleus in the rest frame system will be $E = U + M(A, Z)$, where M is the mass of the nucleus. The total probability per unit time for a nucleus to break up into n components in the final state (*e.g.*, a possible residual nucleus, nucleons, deuterons, tritons, alphas, *etc.*) is given by

$$W(E, n) = (V/\Omega)^{n-1} \rho_n(E), \tag{22}$$

where ρ_n is the density of final states, V is the volume of decaying system and $\Omega = (2\pi\hbar)^3$ is the normalization volume. The density $\rho_n(E)$ can be defined as a product of three factors:

$$\rho_n(E) = M_n(E) S_n G_n. \tag{23}$$

The first one is the phase space factor defined as

$$M_n(E) = \int_{-\infty}^{+\infty} \cdots \int_{-\infty}^{+\infty} \delta\left(\sum_{b=1}^{n} \vec{p}_b\right) \delta\left(E - \sum_{b=1}^{n} \sqrt{p^2 + m_b^2}\right) \prod_{b=1}^{n} d^3 p_b, \tag{24}$$

where $\vec{p}_b$ are fragment momenta. The second one is the spin factor

$$S_n = \prod_{b=1}^{n} (2s_b + 1), \tag{25}$$

which gives the number of states with different spin orientations. The last one is the permutation factor

$$G_n = \prod_{j=1}^{k} \frac{1}{n_j!}, \tag{26}$$

which takes into account identical particles in the final state (n_j is the number of components of j-type particles and k is defined by $n = \sum_{j=1}^{k} n_j$). For example, if we have in the final state six particles ($n = 6$) and two of them are alphas, three are nucleons, and one is a deuteron, then $G_6 = 1/(2!3!1!) = 1/12$. For the non-relativistic case, the integration in Eq. (24) can be evaluated analytically (see, *e.g.*, [36]) and the probability for a nucleus to disintegrate into n fragments with masses m_b, where $b = 1, 2, 3, \ldots, n$ is

$$W(E,n) = S_n G_n \left(\frac{V}{\Omega}\right)^{n-1} \left(\frac{1}{\sum_{b=1}^{n} m_b} \prod_{b=1}^{n} m_b\right)^{3/2} \frac{(2\pi)^{3(n-1)/2}}{\Gamma(3(n-1)/2)} E^{3n/2-5/2}, \qquad (27)$$

where $\Gamma(x)$ is the gamma function.

The angular distribution of n emitted fragments is assumed to be isotropic in the c.m. system of the disintegrating nucleus and their kinetic energies are calculated from the momentum-energy conservation law. The Monte-Carlo method is used to randomly select the decay channel according to probabilities defined by Eq. (27). Then, for a given channel, LAQGSM calculates kinematical quantities for each fragment according to the n-body phase space distribution using Kopylov's method [37]. LAQGSM considers formation of fragments only in their ground and those low-lying states which are stable for nucleon emission. However, several unstable fragments with large lifetimes: ^{5}He, ^{5}Li, ^{9}Be, ^{9}B, *etc.* are considered as well. The randomly chosen channel will be allowed to decay only if the total kinetic energy E_{kin} of all fragments at the moment of break-up is positive, otherwise a new simulation will be performed and a new channel will be selected. The total kinetic energy E_{kin} can be calculated according to the equation:

$$E_{kin} = U + M(A,Z) - E_{Coulomb} - \sum_{b=1}^{n} (m_b + \epsilon_b), \qquad (28)$$

where m_b and ϵ_b are masses and excitation energies of fragments, respectively, and $E_{Coulomb}$ is the Coulomb barrier for the given channel. It is approximated by

$$E_{Coulomb} = \frac{3}{5}\frac{e^2}{r_0}\left(1 + \frac{V}{V_0}\right)^{-1/3} \left(\frac{Z^2}{A^{1/3}} - \sum_{b=1}^{n} \frac{Z_b^2}{A_b^{1/3}}\right), \qquad (29)$$

where A_b and Z_b are the mass number and the charge of the b-th particle of a given channel, respectively. V_0 in the volume of the system corresponding to normal nuclear density and $V = kV_0$ is the decaying system volume ($k = 1$ is assumed in LAQGSM).

Thus, the Fermi break-up model has only one free parameter, V or V_0, the volume of decaying system, which is estimated as follows:

$$V = 4\pi R^3/3 = 4\pi r_0^3 A/3, \qquad (30)$$

where we use $r_0 = 1.3$ fm in LAQGSM. This parameter enters when calculating the quantity VL in the routine CITAB and could be, in principle, changed by users wishing to "play" with LAQGSM.

Note that there is no limitation on the number n of fragments a nucleus may break up into in the version of the break-up model released in LAQGSM, in contrast to implementations in other codes, like $n \leq 3$ in MCNPX, or $n \leq 7$ in LAHET.

2.5. CEM2k model for preequilibrium and evaporation modes

When the mass number(s) of the residual nucleus(i) after the cascade stage of a reaction is(are) larger than 13, LAQGSM uses an improved version [14]–[17] of the Cascade-Exciton Model (CEM) [13] (the code CEM2k [14]) to calculate the preequilibrium and evaporation stages of the reaction after the cascade. All the basic physical ideas, main formulas, and a detailed description of the CEM may be found in Ref. [13]. The new ingredients and refinements incorporated in the recently improved CEM together with a comprehensive comparison with available data and results from other models are described in [14]–[17], therefore we outline here only the main concepts of the preequilibrium and evaporation parts of CEM2k [14] used in LAQGSM and their difference from the original version of CEM [13]

At the preequilibrium stage of a reaction the CEM takes into account all possible nuclear transitions changing the number of excitons n with $\Delta n = +2, -2$, and 0, as well as all possible multiple subsequent emissions of n, p, d, t, ^{3}He, and ^{4}He. The corresponding system of master equations describing the behavior of a nucleus at the preequilibrium stage is solved by the Monte-Carlo technique. Let us note that in the CEM the initial configuration for the preequilibrium decay (number of excited particles and holes, *i.e.* excitons $n_0 = p_0 + h_0$, excitation energy E_0^*, linear momentum $\vec{P}_0$ and angular momentum $\vec{L}_0$ of the nucleus) differs significantly from that usually postulated in most other exciton models.

The CEM predicts forward-peaked (in the laboratory system) angular distributions for preequilibrium particles (in addition to the high asymmetry of the cascade component of LAQGSM). A possibility for forward-peaked distributions of nucleons and composite particles emitted during the preequilibrium interaction stage is related to retention of some memory of the projectile's direction. It means that along with energy conservation we need to take into account the conservation of linear momentum $\vec{P}_0$ at each step when a nuclear state is getting complicated. In the CEM, this is accomplished by sharing the incoming (from the cascade stage) momentum $\vec{P}_0$ (similarly to energy E_0^*) between an ever-increasing number of excitons interacting in the course of equilibration of the nuclear system. In other words, the momentum $\vec{P}_0$ should be attributed only to n excitons rather than to all A nucleons. Then, particle emission will be symmetric in the rest frame of the n-exciton system, but will have some forward peaking in both the laboratory and center-of-mass reference frames.

By "preequilibrium particles" we mean particles which have been emitted after the cascade stage of a reaction but before achieving statistical equilibrium at a time t_{eq}, which is fixed by the condition that transition rates in the direction of increasing the number of excitons and in opposite direction have equal probabilities, $\lambda_+(n_{eq}, E) = \lambda_-(n_{eq}, E)$, from which we get for the number of excitons of an equilibrated system $n_{eq} \simeq \sqrt{2gE}$, where g is the single-particle density and E is the excitation energy of the system. At $t \geq t_{eq}$ (or $n \geq n_{eq}$), the behavior of the remaining excited compound nucleus is described in the framework of both the Weisskopf-Ewing statistical theory of particle evaporation and fission competition according to the Bohr-Wheeler theory.

To be able to analyze reactions with heavy targets and to describe accurately excitation functions over a wide range of incident particle energy, the CEM has been extended from its original form [17]. The extended version incorporates the competition between evaporation and fission of compound nuclei, takes into account pairing energies, considers the angular momentum of preequilibrium and evaporated particles and the rotational energy of excited nuclei, and can use more realistic nuclear level densities (with Z, N, and E^* dependence

of the level-density parameter). The extended version of the CEM contained in the code CEM95 is described in detail in Ref. [17].

The improved cascade-exciton model contained in the code CEM97 [15, 16] differs from the CEM95 version by incorporating new and better approximations for the elementary cross sections in the cascade, using more precise values for nuclear masses, Q-values, binding and pairing energies, using corrected systematics for the level-density parameters, including the Pauli principle in the pre-equilibrium calculation, and a number of important improvements for the cascade stage of reactions, which are not employed in LAQGSM (which uses DCM instead of CEM2k to describe the cascade).

CEM97 also has a number of refinements in comparison with CEM95 in the calculation of the fission channel, described separately in Ref. [16]. In addition, many algorithms used in the Monte-Carlo simulations in many subroutines have been improved, decreasing the computing time by up to a factor of 6 for heavy targets, which is very important when performing practical calculations.

CEM2k [14] is a further improvement of the CEM; it differs from CEM97 mainly in the details of the transitions from the cascade stage of a reaction to the preequilibrium one, and in the duration of the preequilibrium stage. This preliminary version of CEM2k has less preequilibrium emission than the earlier versions. These changes were motivated by discrepancies with the recent GSI data [38] found with the earlier versions of the CEM. These changes provide a higher yield of neutrons, and as a result, a much better agreement with all GSI and other measurements on nuclide yields. Also, reduced masses of particles in the calculation of their emission widths are incorporated into CEM2k instead of using the approximation of no recoil used in previous versions of CEM. This change increases only slightly the agreement of calculated nuclide production yields with the GSI and other available data on heavy targets, but are very important for a correct description of alpha and other complex particle emission, especially from light targets: CEM2k provides a reasonable agreement of alpha particle yields from light and medium targets with available data, while previous versions of the CEM showed a consistent underprediction by a factor of 2 to 3.

CEM2k is surveyed in [14], it is still under development (when completed, it will replace the present version of CEM2k in LAQGSM), nevertheless, even the present preliminary version incorporated into LAQGSM provides a much better agreement with available data than previous versions CEM95 and CEM97.

Note that as the fission model in CEM2k is still under development and does not yet provide production of fission fragments, we have disabled the fission channel in the present version of LAQGSM. If it is necessary to take into account competition between particle evaporation and the fission mode when calculating with LAQGSM a reaction on a heavy target, users may replace the statement "idel = 0" with "idel = 1" in the subroutine INIPREC: this will allow the code to calculate fission cross sections and nuclear fissility, but fission fragments will be still not be provided until we replace the present preliminary version of CEM2k in LAQGSM with a more complete one.

At the end of this section let us make several general comments. First, besides a new treatment of preequilibrium and evaporation (with an option of considering fission for heavy nuclei, as mentioned above), in the present version of LAQGSM we make also a number of refinements in comparison with the standard version of the model [8]–[12], like replacing the old random number generator (which was deficient in generating random numbers very

close to 0 and 1) with the universal double-precision random number generator proposed by Marsaglia and Zaman in the report FSU-SCRI-87-50. In addition, we correct several observed small misprints in the old version of the code and change several parameters. We also add several new modes for elementary interactions during the cascade, such as $\pi + N \to \eta + N$, $\pi + \pi \to K + K$, $B + B \to Y + B + K$, where B denotes a baryon and Y denotes a hyperon, *etc.*

We note that the QGSM part of the LAQGSM code is very similar to that in the CERN code GEANT4, described in detail by Nikolai Amelin in [36], as these parts of both codes are based on the same models and were developed by the same authors during their work at JINR, Dubna. Nevertheless there are a number of non-essential differences between these parts of the two codes, like the values of some parameters, the modes of elementary interactions taken into account at the cascade stage, some details in the dynamics of nucleus-nucleus interactions, *etc.* Therefore predictions by the two codes should be similar but not necessarily coincident even for properties with no contribution from preequilibrium and evaporation, which are treated differently by the codes.

As a confirmation of this, we show in Fig. 4 a comparison of π^+, π^-, K^+, and K^-, spectra (which do not contain contributions from preequilibrium or evaporation) from the reaction p(70 GeV) + C calculated with the standard version of the QGSM [8]–[12] (labeled in the figure as QGSM) and with our present code LAQGSM (labeled as LAQGSM) compared with experimental data from Ref. [34] as well as with predictions by the well known codes FLUKA(96) [39] and MARS [40]. One can see that our present version of LAQGSM describes the data better than the standard version of QGSM incorporated in the CERN code GEANT4. Predictions by the FLUKA and MARS codes also agree well with the measurement, though slightly worse than LAQGSM does.

Note that although LAQGSM is intended as a code to solve applied problems at energies of tens to hundreds of GeV, like PRAD [1], it also works very well at intermediate energies of about 1 GeV and below; therefore, it may be used as well in applications at intermediate energies like Accelerator Transmutation of nuclear Wastes (ATW), National Spallation Neutron Source (NSNS), Rear Isotope Accelerator (RIA), *etc.* An example of LAQGSM 's applicability at GeV energies is shown in Fig. 5, where we compare experimental [41] neutron spectra from interactions of 1.5 and 0.8 GeV protons with lead to calculations by LAQGSM and by CEM97 [15, 16] and CEM2k [14] codes. LAQGSM describes these data as well as CEM97 and CEM2k do.

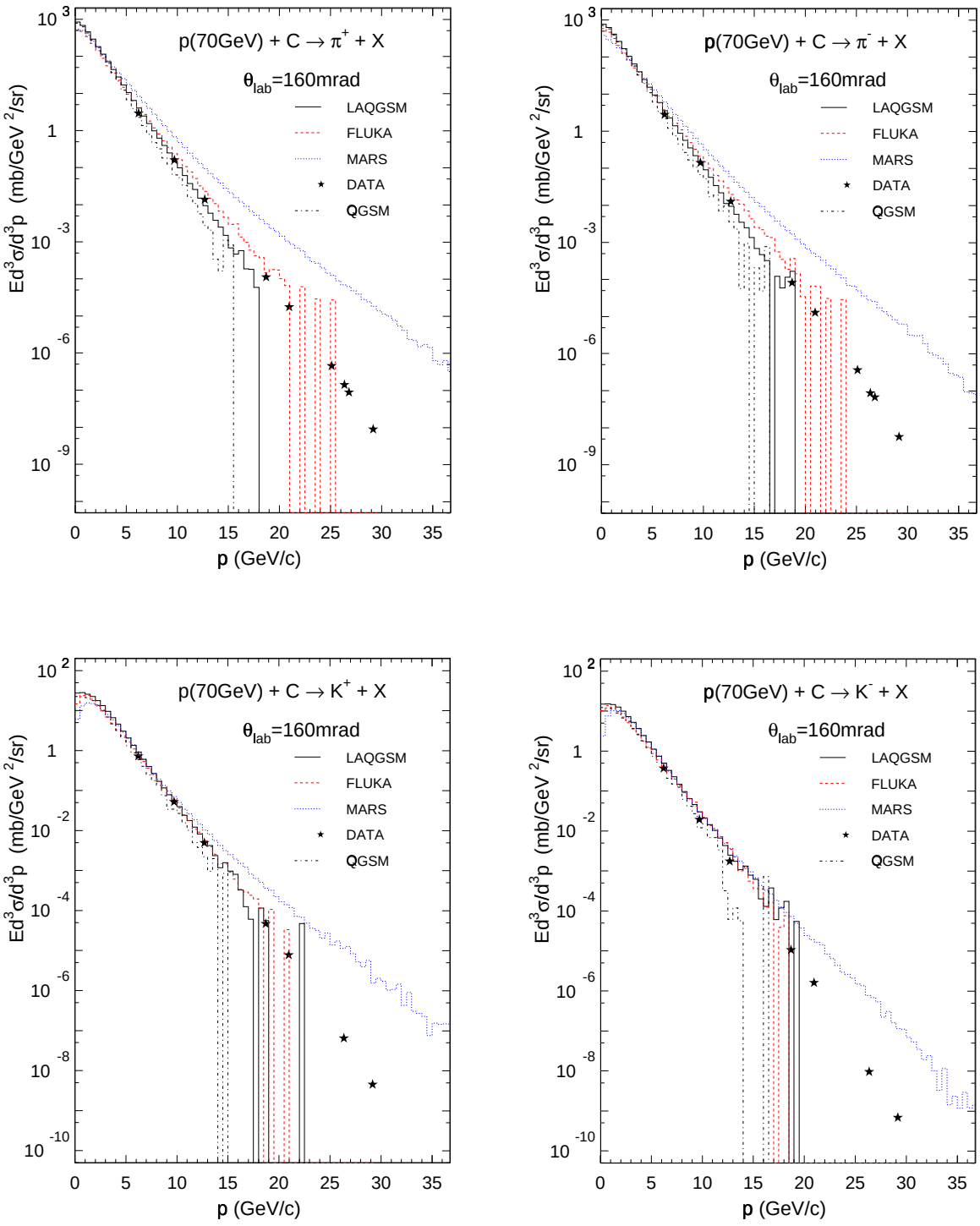

Figure 4: Comparison of the invariant cross sections $Ed^3\sigma/d^3p$ for production of π^+, π^-, K^+, K^- from p + C collisions at 70 GeV as functions of particle momentum p calculated by the current version of LAQGSM with results from the standard version of QGSM [8–12] and with the experimental data from [34], as well as with results by the FLUKA [39] and MARS [40] codes.

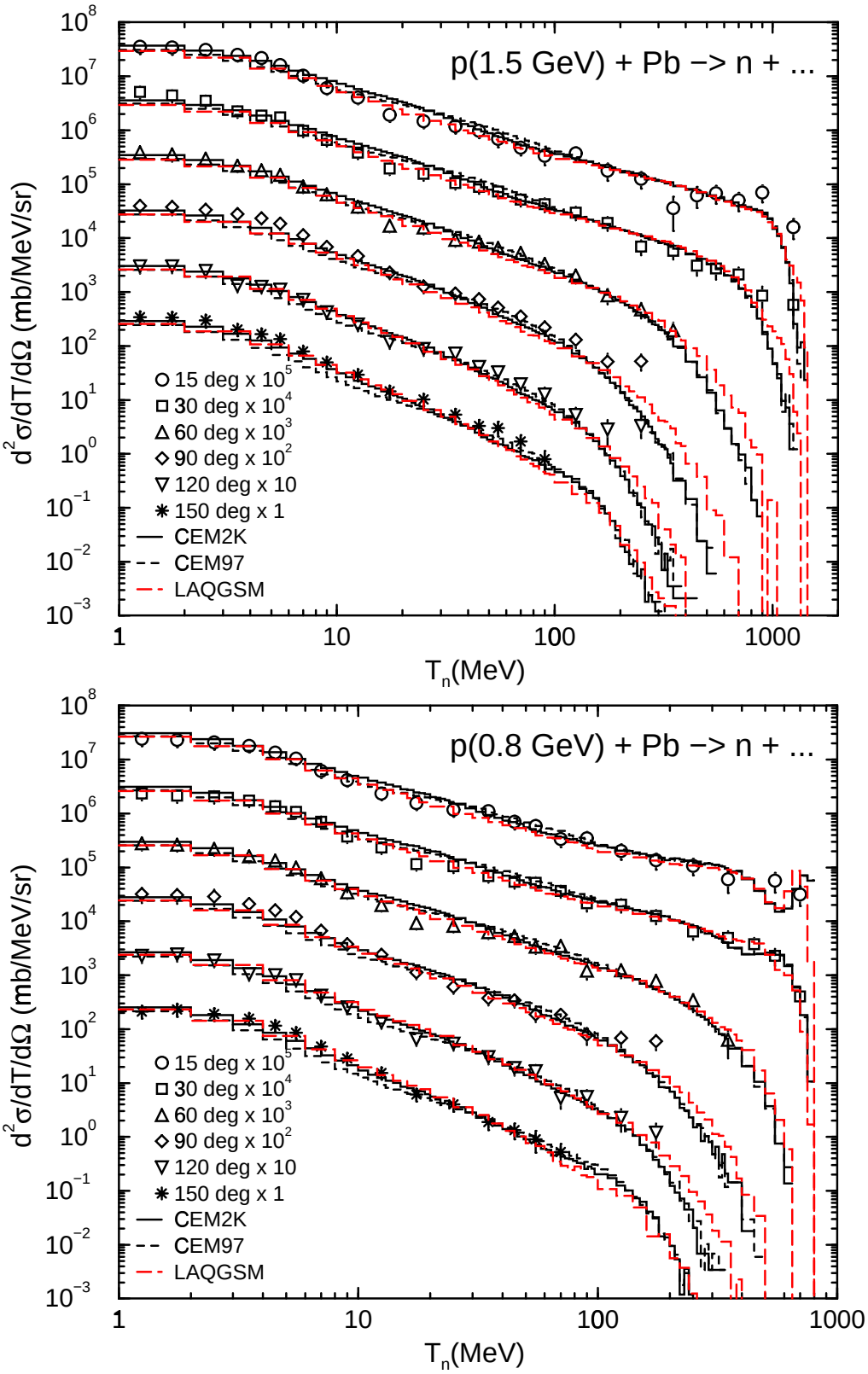

Figure 5: Comparison of measured [41] double differential cross sections of neutrons from 1.5 and 0.8 GeV protons on Pb with LAQGSM results and CEM2k and CEM97 calculations from Ref. [14].

3. Main Parameters and Storage of Results of a Calculation

All explicit input parameters needed to calculate a hadron- or nucleus-nucleus reaction are described in the next section. But as in other models, LAQGSM has a number of fixed, implicit parameters, which may be changed, in principle, by a user wishing to modify and develop further the code. We outline below a number of these parameters:

First, let us mention that collisions of two cascade particles may take place either inside the bombarding and target nuclei and or outside them. To limit to a reasonable value the time of tracing trajectories outside the target and bombarding nuclei for cascade particles with almost parallel momenta (therefore with a non-zero probability of interaction) far beyond the nuclei (see Eqs. (15,16)), the model uses a parameter t_{cas}^{lim} defined by the quantity TLIMIT in the subroutine INITGU. In LAQGSM, $t_{cas}^{lim} = 100$ fm/c, meaning that cascade particles are traced both inside and outside the interacting nuclei, but only during a time of 100 fm/c starting from the beginning of a reaction; after this, all cascade particles are treated as "free" and the cascade stage of the reaction is considered completed. Our experience shows that using a longer t_{cas}^{lim} will have almost no effect on the final results, but the total computing time of LAQGSM will increase considerably.

Another implicit parameter of LAQGSM is the hadron formation time, t_f^0, discussed in the previous section. LAQGSM uses as a default $t_f^0 = c_\tau \hbar / m_\pi$ fm/c, with $c_\tau = 1.0$ for mesons and $c_\tau = 0$, for baryons. These values are defined by the quantities MMES and MBAR in the subroutine INITGU. We do not recommend changing the value of MBAR, while the value of MMES may, in principle, be changed to describe better some experimental data. Note that using a lower value for MMES, *e.g.*, of 0.1, will only increase slightly the multiplicity of produced mesons (see Table 1) and change a little the calculated meson spectra (see Figs. 2 and 3), but will increase several times the computing time of the code, therefore we do not recommend such exercises with LAQGSM for applied problems.

Another implicit parameter of LAQGSM is x_{max}^b, defined by the quantity XBMAX in the same subroutine INITGU. It determines the range of simulated impact parameter, b, for the bombarding hadron or nucleus with the target nucleus, $0 \le b \le x_{max}^b \cdot b_{max}$, where b_{max} is the maximum possible impact parameter. This allows study, *e.g.*, of only central or peripherical collisions. To simulate all possible impact parameters, we should use $x_{max}^b = 1$, as given by default in LAQGSM. But if we wixh to simulate interactions of two nuclei at a given impact parameter, we should change XBMAX in the subroutine INITGU; for instance, to simulate only central collisions, we will need to use XBMAX = 0. In order to restrict consideration to peripheral collisions, it would be necessary to modify the code to insert a minimum x ¿ 0.

There are many other fixed parameters in LAQGSM, but we suggest users first contact the authors before changing their default values.

The present version of the code LAQGSM provides in its output file the total number of elastic and inelastic simulated events, the inelastic cross section, the multiplicity of secondary p, n, d, t, ^{3}He, ^{4}He, π^+, π^-, K^+, K^-, and $\bar{p}$ and their double differential cross sections for up to 10 angles either in the invariant form, $Ed^3\sigma/d^3p$ as a function of the momentum p of the detected particle, or as $d^2\sigma/dT/d\Omega$ as a function of the particle kinetic energy T, and/or (depending on the input parameter INSP, see the next section) in a non-normalized form, *i.e.*, as distributions of the number of produced particles at a given angle as functions of their momenta. Results of calculations may be obtained either in the Laboratory System (LS), in the Center-of-Mass System (CMS), or in the Equal-Velocity System (ECS) (depending on

the input parameter ISYS, see the next section), taking into account contributions either only from the cascade stage, or from the cascade followed by the preequilibrium and evaporation stages for all residual nuclei, or from the cascade followed by the preequilibrium and evaporation stages for residual nuclei after the cascade with $A > 13$ and from the cascade followed by the Fermi break-up for residual nuclei after the cascade with $A \leq 13$, or as in the last case plus contributions from coalescence of complex particles after the cascade (depending on the input parameter JJJ, see the next section).

But even with such a versatile output, some users will need information about more/other types of particles emitted in a reaction or completely different characteristics of a reaction rather then the ones mentioned above. To help users in writing their own routines to obtain with LAQGSM the needed output or to incorporate LAQGSM into a transport code like LAHET or MCNPX, we provide below detailed information about the arrays where all characteristics of a simulated reaction are stored by the code.

All the information about all MV produced particles and residual nuclei (there may be two residual nuclei in the case of A+A interactions) after each nonelastic simulated event is stored in the array UP1 (see the common block UPAC in the subroutine SPECTR). The notation is as follows:

1. P1(LU − 10) is the electric charge of the particle (or residual nucleus),
2. P1(LU − 9) is the strangeness,
3. P1(LU − 8) is the baryon number,
4. P1(LU − 7) is the mass (in GeV),
5. P1(LU − 6) is the X coordinate (in fm) of the last interaction (production) in the "observer" system (the "observer" system is the system where real calculations are done by LAQGSM; it depends on the value of the parameter KSYST defined in the subroutine INITGU and is the LS, if KSYST=1, ECS for KSYST=2, and CMS for KSYST=3; the default "observer" system in the present version of LAQGSM is the Laboratory System (LS)),
6. P1(LU − 5) in the Y coordinate defined in the same manner as X,
7. P1(LU − 4) in the Z coordinate defined in the same manner as X and Y,
8. P1(LU − 3) is the x-component of the particle momentum, p_x, in GeV/c in the system of reference chosen for the final results (*e.g.*, LS, if the input parameter ISYS = 1, 2, or 3; see the next section),
9. P1(LU − 2) in the p_y defined in the same manner as p_x,
10. P1(LU − 1) in the p_z defined in the same manner as p_x and p_y,
11. P1(LU) is the weight for the particular traced particle (equal to one for all particles in the present version of LAQGSM),

where LU=11*M, M=1, 2, ..., MV, and MV is the total number of produced particles and residual nuclei.

To identify a particle stored in the array UP1 for a given value of LU one may either look at its mass, charge, strangeness, and baryon number, or one may instead use the identification number stored for each LU in the array IDPME (see subroutine SPECTR). Table 2 shows the identification numbers for all types of particles considered in the present version of LAQGSM. For nucleons and fragments produced from the preequilibrium, evaporation, or Fermi decay modes of a reaction, the identification number is assigned as zero, IDPME(M)=0.

Table 2: Identification numbers of all secondary particles considered by LAQGSM

Particle Table Number	Particle Label	Identification number
1	π^+	120
2	π^-	-120
3	K^+	130
4	K^-	-130
5	K^0	230
6	$\bar{K}^0$	-230
7	π^0	110
8	η	220
9	η'	330
10	ρ^+	121
11	ρ^-	-121
12	K^{*+}	131
13	K^{*-}	-131
14	K^{*0}	231
15	$\bar{K}^{*0}$	-231
16	ρ	111
17	ω	221
18	ϕ^0	331
19	$\bar{p}$	-1120
20	$\bar{n}$	-1220
21	$\bar{\Sigma}^+$	-1130
22	$\bar{\Sigma}^-$	-2230
23	$\bar{\Sigma}^0$	-1230
24	$\bar{\Xi}^-$	-2330
25	$\bar{\Xi}^0$	-1330
26	$\bar{\Lambda}$	-2130
27	$\bar{\Delta}^{++}$	-1111
28	$\bar{\Delta}^+$	-1121
29	$\bar{\Delta}^-$	-2221
30	$\bar{\Delta}^0$	-1221
31	$\bar{\Sigma}^{*+}$	-1131
32	$\bar{\Sigma}^{*-}$	-2231

Table 2 (continued)

Particle Table Number	Particle Label	Identification number
33	$\bar{\Sigma}^{*0}$	-1231
34	$\bar{\Xi}^{*-}$	-2331
35	$\bar{\Xi}^{*0}$	-1331
36	$\bar{\Omega}^{-}$	-3331
37	p	1120
38	n	1220
39	Σ^{+}	1130
40	Σ^{-}	2230
41	Σ^{0}	1230
42	Ξ^{-}	2330
43	Ξ^{0}	1330
44	Λ	2130
45	Δ^{++}	1111
46	Δ^{+}	1121
47	Δ^{-}	2221
48	Δ^{0}	1221
49	Σ^{*+}	1131
50	Σ^{*-}	2231
51	Σ^{*0}	1231
52	Ξ^{*-}	2331
53	Ξ^{*0}	1331
54	Ω^{-}	3331
55	K_S	20
56	K_L	-20
57	γ	10
58	e^{-}	12
59	e^{+}	-12
60	μ^{+}	-14
61	μ^{-}	14
62	ν_e	11
63	ν_μ	13
64	$\bar{\nu}_e$	-11
65	$\bar{\nu}_\mu$	-13

We like to mention that it is possible to get results of LAQGSM calculations not only for the sum of all modes of a reaction but also separately for the contributions from the different stages. For this, users may easily write their own routines using the information about the array IORI provided in the comments in the beginning of the subroutine DIFSPE together with the information given in this section.

4. Description of INPUT

The input of LAQGSM consists of 9 records, all unformatted. The present version of LAQGSM requires that after starting to run the code, we type first on the console the name of the input file; then, the code reads the input file. The first 6 lines are read from the main program LAQGSM, while the last 3 lines are read from the subroutine PRSPE1.

4.1. First INPUT Line

This line gives the name of the output file, FOUT, where all the final results of calculation will be written.

4.2. Second and Third INPUT Lines

These lines gives the name of two auxiliary output files, FR10 and FR11, used only by the code to read and write intermediate results to allow for restarts. FR10 is a non-formatted file and FR11 is a formatted file, but both are auxiliary, used only by the code and users do not need to read or print them but should only give them names (see an example in the Appendix).

4.3. Fourth INPUT Line

This line is also auxiliary and shows the name of the file (usually, **atab.dat**) from where LAQGSM reads all the data for particle widths, decays, *etc.* The file **atab.dat** is a part of LAQGSM and should be in the same directory as all other files associated with the code; We do not recommend that users modify the file **atab.dat**.

4.4. Fifth INPUT Line

This line is also auxiliary and shows the particular mode of a run, and was introduced to allow users to do long calculations in several steps, accumulating statistics at each step while providing intermediate results. The present version of LAQGSM works as follows: It starts the calculation of a reaction and simulates a number of inelastic events, storing all the information about all produced particles, residual nuclei, last random number, and some other auxiliary data until this information reaches a size of about 70,000 numbers. Then, the code produces the needed output for this number of simulated events and writes all these preliminary results in "zone" No. 1 of files FR10 and FR11. After that, the code simulates the next number of events and writes the second preliminary results in the zone No. 2 of files FR10 and FR11, and so on, until the number of inelastic simulated events is equal to the value of the input parameter LIMC, defined in the sixth input line (the number of events written in each zone is written together with other auxiliary information on the console while LAQGSM runs). At this point, the code writes the final results of this run in the output file FOUT and stops. After that, users may continue to accumulate the statistics in a second run, starting the following calculation either at the last zone written in files FR10 an FR11, or may repeat the calculation from an earlier zone (*e.g.*, if there are suspicions about some results and one would like to track and print all the information about a specific simulated event). The input parameters of the fifth input line allows users to do such calculations. Two parameters should be defined on the fifth line, JG and STAT. JG should be -1 when starting the simulation of a new reaction; 0, for continuing to accumulate the statistics in a following run of the same reaction, -2, in emergency cases (*e.g.*, when the power was shut down and the run stopped before finishing the expected calculations) to read the preliminary results from FR11, write results in FR10 and FOUT, so that in a following run the statistics could be increased; or, any positive number greater than 0, showing from what zone to continue the

calculation. The parameter STAT should be given as NEW in the beginning of simulation of a reaction, when output files FOUT, FR10, and FR11 do not exist, or as OLD, to continue the accumulation of statistics, when files FOUT, FR10, and FR11 where already created in a previous run of this reaction (users should take care to change the parameter STAT from NEW to OLD when performing the second run of a reaction, otherwise LAQGSM will not run).

4.5. Sixth INPUT Line

This is the only line of the input defining the reaction to be calculated. The 7 input parameters given in this line, ANUCL1, ANUCL2, ZNUCL1, ZNUCL2, STIN, AMIN, T0, and LIMC have the following meaning: ANUCL1 and ANUCL2 are the mass (baryon) numbers of the projectile and target, respectively; ZNUCL1 and ZNUCL2 are the electric charge of the projectile and target, respectively; if ANUCL1 ≤ 1 (*i.e.*, for particle+A interactions), the STIN is the strangeness of the projectile and AMIN in the projectile mass in GeV (for A+A interactions, these input parameters are not used); T0 is the kinetic energy of the projectile in GeV per nucleon in the laboratory system; and LIMC is the number of inelastic events to be simulated in this particular run of the code. (When calculating a reaction with high statistics in several consecutive runs, the value of LIMC should be increased for each run, *e.g.*, for the first run one may use 1,000,000 for LIMC, then increase it to 2,000,000, and so on.)

4.6. Seventh, Eighth, and Ninth INPUT Lines

The last 3 lines of the input file define what kind of quantities should be calculated and written onto the output file FOUT. These lines contain the following parameters: The seventh line determines the input parameters JJJ, ISYS, and INSP. JJJ=1, if one wishes to have spectra and multiplicities of secondary particles only from the cascade mode; JJJ=2, if one wishes contributions from the cascade plus preequilibrium, followed by the evaporation modes for all nuclei; JJJ=3, for contributions from the cascade and preequilibrium followed by the evaporation modes for those residual nuclei remaining after the cascade stage of the reaction with the mass numbers $A > 13$, and from the cascade followed by the Fermi break-up, when residual nuclei remaining after the cascade have mass numbers $A \leq 13$; JJJ=11, 12, and 13 mean the same as JJJ=1, 2, and 3, respectively, but also take into account coalescence of d, t, ^{3}He, and ^{4}He from the fast nucleons emitted at the cascade stage.

The input parameter ISYS chooses the frame of reference for the final results: Laboratory System (LS), Center-of-Mass System (CMS), or Equal-Velocity System (EVS). [1] We should use ISYS=1 to get results in the LS (the observer system is also LS, so no conversion is needed in this case); ISYS=2, to convert results into LS if EVS is the observer system; ISYS=-2, to convert results into EVS if LS is the observer system; ISYS=3, to convert results into LS if CMS is the observer system; ISYS=-3, to convert results into CMS if LS is the observer system.

The input parameter INSP defines the form of calculated particle spectra in the output file: We use INSP=1 to get ejectile spectra in the invariant form, $Ed^3\sigma/d^3p$ in units

[1] Let us repeat that the real calculations by the LAQGSM are done in the "observer" system which may be chosen either as LS, or CMS, or EVS, depending of the value of the parameter KSYS in the subroutine INITGU. The present version of the code has a default value of KSYS=1, which means that LS is the observer system and all calculations are done in LS. We recommend this default option for p+A reactions, but KSYS=2 is better for A+A interactions.

of mb$\times c^3$/GeV^2/sr as functions of the momentum p (in GeV/c) of the detected particle; INSP=2, to get spectra in the usual double-differential cross section form, $d^2\sigma/dT/d\Omega$ in units of mb/GeV/sr, as functions of the particle kinetic energy T (in GeV) (this option also provides angle-integrated spectra $d\sigma/dT$ [mb/GeV/sr], as functions of T [GeV]); INSP=3, to get particle spectra not normalized to the total reaction cross section $d^2N/dp/d\Omega$ in units of particles$\times c$ /GeV/sr as functions of the particle momentum p (in GeV/c), where N in the number of particles with the momentum p emitted at angle Ω per incident projectile. Independently of the kind of spectra we choose (the value of INSP), the output file always provides in the beginning also unnormalized particle distributions (spectra), *i.e.*, tables of numbers of particles produced at angle Ω with the momentum p [GeV/c] (for INSP=1 or 3), or with the kinetic energy T [GeV] (for INSP=2) from all simulated events, which provides an idea about the statistics of the simulation for a particular spectrum.

The eighth line defines the ten angles of emission at which particle spectra are calculated, **theta(10)**, and their angular interval, **dtheta** (in units of deg.)).

The ninth line determines the momentum steps in GeV/c, if INSP=1 or 3, or the kinetic energy steps in GeV, if INSP=2, to be used in particle spectra at the ten angles defined in the previous input line, **dp(10)**, and the lowest value of particle momentum [GeV/c] or kinetic energy [GeV] to start calculation of spectra, **pmin** (usually, 0). After the ninth input line, any lines with comments may be added, as they will not be written by LAQGSM.

An example of the INPUT file for LAQGSM is shown in the Appendix.

5. Description of the OUTPUT

We hope that the output of LAQGSM is clear to users with few explanations; nevertheless, let as comment briefly on the example shown in the Appendix.

In the beginning of the output the main information from the input file is printed, to remind us what case is shown in this particular output file. The first five lines contain the names of the input file and its parameters FOUT, FR10, FR11, and atab.dat. Then follows the values of the input parameters JG and STAT, indicating that these are results from a first run of the code for this particular reaction (JG=-1), and that we started the calculations without having any output files for our case (STAT=NEW). Then, we see that we ran the version of LAQGSM of June 15, 2001. The next three output lines show us that this are results for the reaction p(70 GeV) + ^{27} Al. The next four lines give values of several default parameters of LAQGSM and are not of interest to users. The following line is also not of interest in this case as it shows that the strangeness of the projectile is zero (STMIN=0) and its mass is of 0.94 GeV (AMIN=0.940), that is of course for the incident protons. The following line shows that the results of this calculation begin with the first zone of files FR10 and FR11, as described in Sec. 4.4 above, (START NZON = 1), and that the numbers of previously simulated inelastic and elastic events, respectively, for this reaction were zero (NCAS = 0 and INTEL = 0).

Then we see that these results are in the Laboratory System and that cascade + coalescence + preequilibrium + evaporation + Fermi break-up mechanisms were taken into account in the calculations. Then, we have the value of the geometrical cross section (1177.31 mb), the number of inelastic (10000) and elastic (15062) simulated events, and the total inelastic cross section (469.762 mb).

Further, the information about emitted particles follows: the total number of emitted π^-, π^+, n, p, d, t, ^{3}He, ^{4}He, K^+, K^-, and $\bar{p}$, then, the distribution of these particles with their kinetic energy and emission angle for the ten angles of 0, 4.75, 9.0, 13.0, 20.0, 30.0, 45.0, 60.0, 90.0, and 159.0 degrees given in the input file with the steps in the kinetic energy of particles at each angle as defined in the input file.

The angle-integrated distributions (non-normalized spectra) of the produced particles are given, followed by their multiplicities.

After this, double-differential cross sections, $d^2\sigma/dT/d\Omega$, for all particles at all angles are printed in units of mb/GeV/sr, followed by the angle-integrated spectra, $d\sigma/dT$, in mb/GeV.

Near the end of the output file the fission cross section for this reaction is printed (no fission is taken into account by default in this version of LAQGSM, therefore the fission cross section is zero).

The last two lines of the output show us that this calculation was done in 0 hours 3 minutes and 48 seconds, and that the mean duration of the simulation of an inelastic event for this case was of 0.023 sec.

6. Acknowledgments

We thank all our colleagues and friends, especially Drs. N. S. Amelin, V. D. Toneev, and S. Yu. Sivoklokov, in collaboration with whom were developed most of the models and codes incorporated into LAQGSM. We are grateful to Drs. M. B. Chadwick, R. E. MacFarlane, R. E. Prael, D. D. Strottman, and L. S. Waters for fruitful discussions, interest, and support during the creation of this version of the code LAQGSM at LANL.

This manual was written and the code LAQGSM was completed under the auspices of the U.S. Department of Energy by the Los Alamos National Laboratory under contract W-7405-ENG-36.

References

[1] Christopher L. Morris, "Prpton Radiography for an Advanced Hydrotest Facility," Los Alamos National Laboratory Report LA-UR-00-5716, Los Alamos (2000).

[2] K. K. Gudima and V. D. Toneev, "Have Shock Waves Been Observed in Nuclear Collisions," Sov. J. Nucl. Phys. **27** (1978) 351–357 [Yad. Fiz. **27** (1978) 658–669].

[3] K. K. Gudima and V. D. Toneev, "High-Energy Nuclear Collisions: Evolution of the Compressed Zone," J. Phys. G: Nucl. Phys. **5** (1979) 229–240.

[4] K. K. Gudima and V. D. Toneev, "Extreme Conditions Attainable in High-Energy Nuclear Collisions," Sov. J. Nucl. Phys. **31** (1980) 755–758 [Yad. Fiz. **31** (1980) 1455–1461].

[5] V. D. Toneev and K. K. Gudima, "Particle Emission in Light and Heavy-Ion Reactions," Nucl. Phys. **A400** (1983) 173c–190c.

[6] V. D. Toneev and K. K. Gudima, "Particle Production in Heavy-Ion Collisions at Intermediate Energies," GSI Preprint GSI-93-52, Darmstadt (1993).

[7] N. S. Amelin, "Simulation of Nuclear Collisions at High Energy in the Framework of the Quark-Gluon String Model," Joint Institute for Nuclear Research Report JINR-86-802, Dubna (1986).

[8] V. D. Toneev, N. S. Amelin, and K. K. Gudima, "The Independent Quark-Gluon String Model for Heavy-Ion Collisions at Ultrarelativistic Energies," GSI Preprint GSI-89-52, Darmstadt (1989).

[9] N. S. Amelin, K. K. Gudima, and V. D. Toneev, "The Quark-Gluon String Model and Ultrarelativistic Heavy-Ion Collisions," Sov. J. Nucl. Phys. **51** (1990) 327–333 [Yad. Fiz. **51** (1990) 512–523].

[10] V. D. Toneev, N. S. Amelin, K. K. Gudima, and S. Yu. Sivoklokov, "Dynamics of Relativistic Heavy-Ion Collisions," Nucl. Phys. **A519** (1990) 463c–478c.

[11] N. S. Amelin, K. K. Gudima, and V. D. Toneev, "Ultrarelativistic Nucleus-Nucleus Collisions in a Dynamical Model of Independent Quark-Gluon Strings," Sov. J. Nucl. Phys. **51** (1990) 1093–1101 [Yad. Fiz. **51** (1990) 1730–1743].

[12] N. S. Amelin, K. K. Gudima, and V. D. Toneev, "Further Development of the Model of Quark-Gluon Strings for the Description of High-Energy Collisions with a Target Nucleus," Sov. J. Nucl. Phys. **52** (1990) 172–178 [Yad. Fiz. **52** (1990) 272–282].

[13] K. K. Gudima, S. G. Mashnik, and V. D. Toneev, "Cascade-Exciton Model of Nuclear Reactions," Nucl. Phys. **A401** (1983) 329–361.

[14] S. Mashnik and A. Sierk, "CEM2k—Recent Developments in CEM," Proc. of the 2000 ANS/ENS Int. Meeting, Embedded Topical Meeting *Nuclear Applications of Accelerator Technology (AccApp00)*, November 12–16, 2000, Washington, DC (USA), American Nuclear Society, La Grange Park, IL, (2001) pp. 328–141; E-print: nucl-th/001164.

[15] Stepan G. Mashnik and Arnold J. Sierk, "Improved Cascade-Exciton Model of Nuclear Reactions," Proc. Fourth Int. Workshop on Simulating Accelerator Radiation Environments (SARE-4), Knoxville, TN, September 13–16, 1998, edited by Tony A. Gabriel, ORNL (1999) pp. 29–51; E-print: nucl-th/9812069.

[16] Arnold J. Sierk and Stepan G. Mashnik, "Modeling Fission in the Cascade-Exciton Model," Proc. Fourth Int. Workshop on Simulating Accelerator Radiation Environments (SARE-4), Knoxville, TN, September 13–16, 1998, edited by Tony A. Gabriel, ORNL (1999) pp. 53–67; E-print: nucl-th/9812070.

[17] S. G. Mashnik, "Cascade-Exciton Model Analysis of Excitation Functions for Proton-Induced Reactions at Low and Intermediate Energies," Izv. RAN, Ser. Fiz. **60** (1996) 73–84 [Bulletin of the Russian Academy of Science, Physics, **60** (1996) 58–67]; S. G. Mashnik, User Manual for the Code CEM95, Joint Institute for Nuclear Research, Dubna, Russia (1995), http://www.nea.fr/abs/html/iaea1247.html.

[18] E. Fermi, "High Energy Nuclear Events", Prog. Theor. Phys. **5** (1950) 570–583.

[19] K. K. Gudima, G. Röpke, H. Schulz, and V. D. Toneev, "The Coalescence Model and Pauli Quenching in High-Energy Heavy-Ion Collisions," Joint Institute for Nuclear Research Report JINR-E2-83-101, Dubna (1983); H. Schulz, G. Röpke, K. K. Gudima, and V. D. Toneev, "The Coalescence phenomenon and the Pauli Quenching in High-Energy Heavy- Ion Collisions," Phys. Lett. B **124** (1983) 458–460.

[20] Y. Yariv and Z. Fraenkel, "Intranuclear Cascade Calculation of High-Energy Heavy-Ion Interactions", Phys. Rev. C **20** (1979) 2227–2243.

[21] Y. Yariv and Z. Fraenkel, "Intranuclear Cascade Calculation of High Energy Heavy-Ion Collisions: Effects of Interactions Between Cascade Particles", Phys. Rev. C **24** (1981) 488–494.

[22] J. Cugnon, D. Kinet, and J. Vandermeulen, "Pion Production in Central High-Energy Nuclear Collisions", Nucl. Phys. **A379** (1982) 553–567.

[23] Zeev Fraenkel, "Review of the Intranuclear Cascade Model for Heavy-Ion Reactions," Nucl. Phys. **A428** (1984) 373c–388c.

[24] A. Capella, U. Sukhatme, and J. Tran Thanh Van, "Soft Multihadron Production from Partonic Structure and Fragmentation Functions, Z. Physik C, Particle and Fields **3** (1980) 329–337.

[25] A. B. Kaidalov, "Quark and Diquark Fragmentation Functions in the Model of Quark-Gluon Strings," Sov. J. Nucl. Phys. **45** (1987) 902–907 [Yad. Fiz. **45** (1987) 1452–1461].

[26] P. E. Volkovitskii, "Preasymptotic Corrections to Pomeron Exchange," Sov. J. Nucl. Phys. **44** (1986) 472–477 [Yad. Fiz. **44** (1986) 729–737].

[27] N. S. Amelin, V. S. Barashenkov, and N. V. Slavin, "Monte-Carlo Simulation of Multiparticle Production in High-Energy Collisions of Hadrons," Sov. J. Nucl. Phys. **40** (1984) 991–996 [Yad. Fiz. **40** (1984) 1560–1569].

[28] N. S. Amelin and A. I. Ostrovidov, "Application of the Quark-Gluon String and Cascading-Baryon Models to the Calculation of Momentum Spectra at 19.2 GeV/c," Sov. J. Nucl. Phys. **50** (1989) 302–305 [Yad. Fiz. **50** (1989) 486–492].

[29] R. D. Field and R. P. Feynman, "A Parametrization of the Properties of Quark Jets," Nucl. Phys. **B136** (1978) 1–76.

[30] N. N. Nikolaev, "Interactions of High-Energy Hadrons, Photons, and Leptons with Nuclei," Sov. J. Part. Nucl. **12** (1981) 63–88 [Fiz. Elem. Chastits At. Yadra **12** (1981) 162–219].

[31] B. Z. Kopeliovich and L. L. Lapidus, in *Proc. of the 6th Balaton Conf. on Nuclear Reactions* (Balatonfüred, 1983), edited by E. Fodor, Budapest (1983), p. 73.

[32] A. Bialas and M. Gyulassy, "Lund Model and an Outside-Inside Aspect of the Inside-Outside Cascade," Nucl. Phys. **B291** (1987) 793–812.

[33] N. S. Amelin, "On the Hadron Formation Time within the Quark-Gluon String Model," Brief Reports on JINR Physics [in Russian], Dubna (1989) Vol. 3, pp. 32–38. [Yad. Fiz. **50** (1989) 486–492].

[34] V. V. Abramov, B. Yu. Baldin, A. F. Buzulutskov, Yu. N. Vrazhnov, V. Yu. Glebov, A. S. Dyshkant, V. N. Evdokimov, A. O. Efimov, V. V. Zmushko, A. N. Krinitsyn, V. I. Kryshkin, N. Yu. Kulman, M. I. Mutafyan, V. M. Podstavkov, R. M. Sulyaev, and L. K. Tuchanovich, "Production of Hadrons with large $P_\perp$ in nuclei at 70 GeV," Sov. J. Nucl. Phys. **41** (1985) 227–236 [Yad. Fiz. **41** (1985) 357–370]; tabulated values of these data are available on the HEPDATA REACTION DATABASE server at: http://durpdg.dur.ac.uk/cdi-bin/hepdata/testreac/.

[35] Joseph I. Kapusta, "Mechanisms for Deuteron Production in Relativistic Nuclear Collisions," Phys. Rev. C **21** (1980) 1301–1310.

[36] Nikolai Amelin, "Physics and Algorithms of the Hadronic Monte-Carlo Event Generators. Notes for a Developer," CERN/IT/ASD Report CERN/IT/99/6, Geneva, Switzerland and JINR/LHE, Dubna, Russia; "GEANT4, Users's Documents, Physics Reference Manual," last update 08/04/99: http://wwwinfo.cern.ch/asd/geant4/G4UsersDocuments/UsersGuides/ PhysicsReferenceManual/html/PhysicsReferenceManual.html.

[37] G. I. Kopylov, *Principles of Resonance Kinematics*, Moscow, Nauka (1970) [in Russian].

[38] W. Wlazlo, T. Enqvist, P. Armbruster, J. Benlliure, M. Bernas, A. Boudard, S. Czájkowski, R. Legrain, S. Leray, B. Mustapha, M. Pravikoff, F. Rejmund, K.-H. Schmidt, C. Stéphan, J. Taieb, L. Tassan-Got, and C. Volant, "Cross Sections of Spallation Residues Produced in 1A GeV ^{208}Pb on Proton Reactions," Phys. Rev. Lett. **84** (2000) 5736–5739.

[39] A. Fasso, A. Ferrari, J. Ranft, and P. R. Sala, "An Update About FLUKA," Proc. of the Second Workshop on Simulating Accelerator Radiation Environments (SARE-2), CERN, Geneva, October 9–11, 1996, edited by G. R. Stevenson, Geneva, Switzerland (1997) pp. 158–170.

[40] N. V. Mokhov, "The MARS Code System User's Guide," Fermilab-FN-628 (1995); N. V. Mokhov and O. E. Krivisheev, "MARS Code Status," Fermilab-Conf-00/181 (2000); http://www-ap.fnal.gov/MARS/.

[41] K. Ishibashi, H. Takada, T. Nakomoto, N. Shigyo, K. Maehata, N. Matsufuji, S. Meigo, S. Chiba, M. Numajiri, Y. Watanabe, T. Nakamura, "Measurement of Neutron-Production Double-Differential Cross Sections for Nuclear Spallation Reaction Induced by 0.8, 1.5 and 3.0 GeV Protons," J. Nucl. Sci. Techn. **34** (1997) 529–537.

Appendix

```
Example of an input (pal70.inp) and an output (pal70.out) LAQGSM files, for
the the reaction p(70 GeV) + Al.

                                *************
                                * test.inp *
                                *************

 2 4 6 8(1)2 4 6 8(1)2 4 6 8(1)2 4 6 8(1)2 4 6 8(1)2 4 6 8(1)2 4 6 8(1)2 4 6 8 0
-------------------------------------------------------------------------------

test.res
test.r10
test.r11
atab.dat
-1, NEW
1.0, 27.0, 1.0, 13.0, 0.0, 0.940,70.000,10000
 13, 1, 2
0.000,4.750,9.000,13.000,20.000,30.000,45.000,60.000,90.000,159.000,2.000
0.500,0.500,0.500,0.200,0.200,0.200,0.100,0.100,0.100,0.050,0.000
 JG,STAT
 AP,AT,ZP,ZT,SP,MP,TO/AP,LIMC
 JJJ,ISYS,INSP
 theta(10),dtheta
 dp(10),pmin
```

```
                              *************
                              * test.res *
                              *************
(To save space, some empty lines of this file ere deleted, as are
the tails of all spectra, keeping only the first 4 lines of each spectrum.)

--------------------------------------------------------------------------------

 test.inp
 test.res
 test.r10
 test.r11
 atab.dat
 JG=  -1 STAT=NEW
  PROGRAM VERSION FROM  06. 15.2001

 ANUCL1=  1. ANUCL2= 27.
 ZNUCL1=  1. ZNUCL2= 13.
 T0= 70.000GEV/NUCLEON
 EPS1=0.007 EPS2=0.007 VPI=0.025
 C1=0.545 C2=0.545 D1=0.05 D2=0.05
 RON1=1.07 RON2=1.07
  DELTA=1.3
 STIN= 0. AMIN= 0.940

          START NZON=     1 NCAS=        0 INTEL=        0

                    CASCAD  +COALES +PRECOMP+FERMI
                    LAB.SYSTEM

          GEOMETR. CROSS SECTION=   1177.317576 mb

     Ncas=   10000 INTel=    15062
     INEL. CROSS SECTION= 0.469762E+03 mb
          Number of produced particles
   PI-MINUS    PI-PLUS   NEUTRONS    PROTONS   DEUTRONS    TRITONS       HE-3       HE-4       K+         K-     ANTIPROT
      33250      36422      47604      47360       8373       2024       1458       9043       2662       1270        247

          Number of produced particles at theta=  0.00+/-  2.00
 T(GeV)    PI-MINUS    PI-PLUS   NEUTRONS    PROTONS   DEUTRONS    TRITONS       HE-3       HE-4       K+         K-     ANTIPROT
  0.2500        32.        33.        25.        27.         3.         1.         0.         5.         0.         2.         0.
  0.7500        56.        74.        13.         9.         0.         0.         0.         0.         4.         0.         1.
  1.2500        80.        86.        16.         8.         0.         0.         0.         0.         4.         0.         0.
  1.7500        83.        97.         7.        15.         0.         0.         0.         0.         6.         2.         1.

          Number of produced particles at theta=  4.75+/-  2.00
 T(GeV)    PI-MINUS    PI-PLUS   NEUTRONS    PROTONS   DEUTRONS    TRITONS       HE-3       HE-4       K+         K-     ANTIPROT
  0.2500       218.       228.       255.       212.        27.         2.         5.        30.        10.         3.         0.
  0.7500       436.       503.       124.       114.         1.         0.         0.         0.        33.        22.         1.
  1.2500       569.       615.       121.       104.         1.         0.         0.         0.        38.        22.         2.
  1.7500       623.       659.        98.       100.         1.         0.         0.         0.        33.        14.         2.

          Number of produced particles at theta=  9.00+/-  2.00
 T(GeV)    PI-MINUS    PI-PLUS   NEUTRONS    PROTONS   DEUTRONS    TRITONS       HE-3       HE-4       K+         K-     ANTIPROT
  0.2500       395.       438.       456.       391.        62.        10.         7.        52.        24.         6.         0.
  0.7500       680.       694.       184.       191.         1.         1.         0.         0.        38.        24.         6.
  1.2500       664.       726.       170.       142.         1.         0.         0.         0.        50.        20.         3.
  1.7500       581.       649.       115.       127.         1.         0.         0.         0.        49.        25.         5.

          Number of produced particles at theta= 13.00+/-  2.00
 T(GeV)    PI-MINUS    PI-PLUS   NEUTRONS    PROTONS   DEUTRONS    TRITONS       HE-3       HE-4       K+         K-     ANTIPROT
  0.1000       104.        91.       394.       386.        71.        14.        16.        63.         7.         2.         0.
  0.3000       234.       252.       157.       159.         2.         0.         0.         0.        13.         6.         0.
  0.5000       271.       273.       128.       123.         0.         0.         0.         0.        14.         5.         1.
  0.7000       275.       306.       111.       102.         1.         0.         0.         0.        23.         8.         0.

          Number of produced particles at theta= 20.00+/-  2.00
 T(GeV)    PI-MINUS    PI-PLUS   NEUTRONS    PROTONS   DEUTRONS    TRITONS       HE-3       HE-4       K+         K-     ANTIPROT
  0.1000       151.       176.       593.       535.        94.        30.        18.       104.         9.         6.         0.
  0.3000       281.       279.       203.       192.         0.         0.         0.         0.        11.         6.         0.
  0.5000       265.       314.       160.       167.         3.         0.         0.         0.        17.         6.         0.
  0.7000       259.       275.       126.       142.         1.         0.         0.         0.        12.         9.         2.

          Number of produced particles at theta= 30.00+/-  2.00
 T(GeV)    PI-MINUS    PI-PLUS   NEUTRONS    PROTONS   DEUTRONS    TRITONS       HE-3       HE-4       K+         K-     ANTIPROT
  0.1000       189.       198.       803.       737.       147.        43.        26.       148.         7.         5.         0.
  0.3000       277.       274.       205.       210.         4.         0.         0.         0.        13.         1.         0.
  0.5000       233.       227.       158.       146.         2.         0.         0.         0.         7.         6.         1.
  0.7000       136.       161.       121.        85.         0.         0.         0.         0.         8.         3.         0.

          Number of produced particles at theta= 45.00+/-  2.00
 T(GeV)    PI-MINUS    PI-PLUS   NEUTRONS    PROTONS   DEUTRONS    TRITONS       HE-3       HE-4       K+         K-     ANTIPROT
  0.0500       111.        97.       831.       798.       197.        42.        36.       221.         1.         0.         0.
  0.1500       108.       116.       177.       148.         9.         2.         3.         0.         5.         4.         0.
  0.2500       102.       105.       125.       115.         1.         0.         0.         1.         4.         5.         0.
  0.3500        71.        91.        81.        69.         0.         0.         0.         0.         4.         3.         0.

          Number of produced particles at theta= 60.00+/-  2.00
 T(GeV)    PI-MINUS    PI-PLUS   NEUTRONS    PROTONS   DEUTRONS    TRITONS       HE-3       HE-4       K+         K-     ANTIPROT
  0.0500       106.        95.      1043.       893.       238.        75.        43.       299.         2.         2.         0.
  0.1500        96.        77.       194.       158.        10.         2.         3.         1.         4.         0.         0.
```

0.2500	86.	73.	94.	85.	2.	1.	0.	0.	2.	2.	0.
0.3500	41.	42.	49.	43.	2.	0.	0.	0.	2.	1.	0.

Number of produced particles at theta= 90.00+/- 2.00

T(GeV)	PI-MINUS	PI-PLUS	NEUTRONS	PROTONS	DEUTRONS	TRITONS	HE-3	HE-4	K+	K-	ANTIPROT
0.0500	82.	91.	1035.	1007.	294.	79.	49.	308.	2.	0.	0.
0.1500	46.	65.	91.	64.	2.	1.	0.	4.	1.	0.	0.
0.2500	28.	25.	23.	16.	0.	0.	0.	0.	0.	0.	0.
0.3500	12.	4.	10.	4.	0.	0.	0.	0.	0.	0.	0.

Number of produced particles at theta=159.00+/- 2.00

T(GeV)	PI-MINUS	PI-PLUS	NEUTRONS	PROTONS	DEUTRONS	TRITONS	HE-3	HE-4	K+	K-	ANTIPROT
0.0250	9.	12.	298.	257.	87.	22.	14.	121.	0.	0.	0.
0.0750	14.	13.	40.	18.	8.	5.	2.	1.	0.	0.	0.
0.1250	4.	3.	9.	5.	1.	0.	0.	0.	0.	0.	0.
0.1750	2.	4.	2.	0.	1.	1.	0.	0.	0.	0.	0.

Angle inegrated number of produced particles

T(GeV)	PI-MINUS	PI-PLUS	NEUTRONS	PROTONS	DEUTRONS	TRITONS	HE-3	HE-4	K+	K-	ANTIPROT
0.2500	10335.	10807.	38410.	36321.	8327.	2023.	1458.	9043.	400.	190.	5.
0.7500	5040.	5561.	2765.	2555.	22.	1.	0.	0.	307.	143.	17.
1.2500	3115.	3456.	1297.	1154.	11.	0.	0.	0.	276.	125.	12.
1.7500	2280.	2485.	754.	725.	6.	0.	0.	0.	214.	94.	13.

Multiplicity of produced particles

PI-MINUS	PI-PLUS	NEUTRONS	PROTONS	DEUTRONS	TRITONS	HE-3	HE-4	K+	K-	ANTIPROT
3.3250E+00	3.6422E+00	4.7604E+00	4.7360E+00	8.3730E-01	2.0240E-01	1.4580E-01	9.0430E-01	2.6620E-01	1.2700E-01	2.4700E-02

Spectra (dS/dT/dΩ) of produced particles at theta= 0.00+/- 2.00

T(GeV)	PI-MINUS	PI-PLUS	NEUTRONS	PROTONS	DEUTRONS	TRITONS	HE-3	HE-4	K+	K-	ANTIPROT
0.2500	7.8550E+02	8.1005E+02	6.1367E+02	6.6277E+02	7.3641E+01	2.4547E+01	0.0000E+00	1.2273E+02	0.0000E+00	4.9094E+01	0.0000E+00
0.7500	1.3746E+03	1.8165E+03	3.1911E+02	2.2092E+02	0.0000E+00	0.0000E+00	0.0000E+00	0.0000E+00	9.8188E+01	0.0000E+00	2.4547E+01
1.2500	1.9638E+03	2.1110E+03	3.9275E+02	1.9638E+02	0.0000E+00	0.0000E+00	0.0000E+00	0.0000E+00	9.8188E+01	0.0000E+00	0.0000E+00
1.7500	2.0374E+03	2.3811E+03	1.7183E+02	3.6820E+02	0.0000E+00	0.0000E+00	0.0000E+00	0.0000E+00	1.4728E+02	4.9094E+01	2.4547E+01

Spectra (dS/dT/dΩ) of produced particles at theta= 4.75+/- 2.00

T(GeV)	PI-MINUS	PI-PLUS	NEUTRONS	PROTONS	DEUTRONS	TRITONS	HE-3	HE-4	K+	K-	ANTIPROT
0.2500	5.6398E+02	5.8985E+02	6.5970E+02	5.4846E+02	6.9851E+01	5.1741E+00	1.2935E+01	7.7612E+01	2.5871E+01	7.7612E+00	0.0000E+00
0.7500	1.1280E+03	1.3013E+03	3.2080E+02	2.9492E+02	2.5871E+00	0.0000E+00	0.0000E+00	0.0000E+00	8.5373E+01	5.6915E+01	2.5871E+00
1.2500	1.4720E+03	1.5910E+03	3.1303E+02	2.6905E+02	2.5871E+00	0.0000E+00	0.0000E+00	0.0000E+00	9.8308E+01	5.6915E+01	5.1741E+00
1.7500	1.6117E+03	1.7049E+03	2.5353E+02	2.5871E+02	2.5871E+00	0.0000E+00	0.0000E+00	0.0000E+00	8.5373E+01	3.6219E+01	5.1741E+00

Spectra (dS/dT/dΩ) of produced particles at theta= 9.00+/- 2.00

T(GeV)	PI-MINUS	PI-PLUS	NEUTRONS	PROTONS	DEUTRONS	TRITONS	HE-3	HE-4	K+	K-	ANTIPROT
0.2500	5.4093E+02	5.9982E+02	6.2447E+02	5.3545E+02	8.4906E+01	1.3694E+01	9.5862E+00	7.1211E+01	3.2867E+01	8.2167E+00	0.0000E+00
0.7500	9.3123E+02	9.5040E+02	2.5198E+02	2.6156E+02	1.3694E+00	1.3694E+00	0.0000E+00	0.0000E+00	5.2039E+01	3.2867E+01	8.2167E+00
1.2500	9.0931E+02	9.9422E+02	2.3281E+02	1.9446E+02	1.3694E+00	0.0000E+00	0.0000E+00	0.0000E+00	6.8473E+01	2.7389E+01	4.1084E+00
1.7500	7.9565E+02	8.8877E+02	1.5749E+02	1.7392E+02	1.3694E+00	0.0000E+00	0.0000E+00	0.0000E+00	6.7103E+01	3.4236E+01	6.8472E+00

Spectra (dS/dT/dΩ) of produced particles at theta= 13.00+/- 2.00

T(GeV)	PI-MINUS	PI-PLUS	NEUTRONS	PROTONS	DEUTRONS	TRITONS	HE-3	HE-4	K+	K-	ANTIPROT
0.1000	2.4761E+02	2.1666E+02	9.3805E+02	9.1901E+02	1.6904E+02	3.3332E+01	3.8094E+01	1.4999E+02	1.6666E+01	4.7617E+00	0.0000E+00
0.3000	5.5712E+02	5.9997E+02	3.7379E+02	3.7855E+02	4.7617E+00	0.0000E+00	0.0000E+00	0.0000E+00	3.0951E+01	1.4285E+01	0.0000E+00
0.5000	6.4521E+02	6.4997E+02	3.0475E+02	2.9284E+02	0.0000E+00	0.0000E+00	0.0000E+00	0.0000E+00	3.3332E+01	1.1904E+01	2.3808E+00
0.7000	6.5473E+02	7.2854E+02	2.6427E+02	2.4285E+02	2.3808E+00	0.0000E+00	0.0000E+00	0.0000E+00	5.4759E+01	1.9047E+01	0.0000E+00

Spectra (dS/dT/dΩ) of produced particles at theta= 20.00+/- 2.00

T(GeV)	PI-MINUS	PI-PLUS	NEUTRONS	PROTONS	DEUTRONS	TRITONS	HE-3	HE-4	K+	K-	ANTIPROT
0.1000	2.3645E+02	2.7560E+02	9.2859E+02	8.3776E+02	1.4720E+02	4.6977E+01	2.8186E+01	1.6285E+02	1.4093E+01	9.3955E+00	0.0000E+00
0.3000	4.4002E+02	4.3689E+02	3.1788E+02	3.0065E+02	0.0000E+00	0.0000E+00	0.0000E+00	0.0000E+00	1.7225E+01	9.3955E+00	0.0000E+00
0.5000	4.1497E+02	4.9170E+02	2.5055E+02	2.6151E+02	4.6977E+00	0.0000E+00	0.0000E+00	0.0000E+00	2.6620E+01	9.3955E+00	0.0000E+00
0.7000	4.0557E+02	4.3063E+02	1.9730E+02	2.2236E+02	1.5659E+00	0.0000E+00	0.0000E+00	0.0000E+00	1.8791E+01	1.4093E+01	3.1318E+00

Spectra (dS/dT/dΩ) of produced particles at theta= 30.00+/- 2.00

T(GeV)	PI-MINUS	PI-PLUS	NEUTRONS	PROTONS	DEUTRONS	TRITONS	HE-3	HE-4	K+	K-	ANTIPROT
0.1000	2.0245E+02	2.1209E+02	8.6013E+02	7.8944E+02	1.5746E+02	4.6059E+01	2.7850E+01	1.5853E+02	7.4980E+00	5.3557E+00	0.0000E+00
0.3000	2.9671E+02	2.9349E+02	2.1959E+02	2.2494E+02	4.2846E+00	0.0000E+00	0.0000E+00	0.0000E+00	1.3925E+01	1.0711E+00	0.0000E+00
0.5000	2.4958E+02	2.4315E+02	1.6924E+02	1.5639E+02	2.1423E+00	0.0000E+00	0.0000E+00	0.0000E+00	7.4980E+00	6.4269E+00	1.0711E+00
0.7000	1.4568E+02	1.7245E+02	1.2961E+02	9.1048E+01	0.0000E+00	0.0000E+00	0.0000E+00	0.0000E+00	8.5692E+00	3.2134E+00	0.0000E+00

Spectra (dS/dT/dΩ) of produced particles at theta= 45.00+/- 2.00

T(GeV)	PI-MINUS	PI-PLUS	NEUTRONS	PROTONS	DEUTRONS	TRITONS	HE-3	HE-4	K+	K-	ANTIPROT
0.0500	1.6815E+02	1.4694E+02	1.2588E+03	1.2088E+03	2.9842E+02	6.3623E+01	5.4534E+01	3.3478E+02	1.5148E+00	0.0000E+00	0.0000E+00
0.1500	1.6360E+02	1.7572E+02	2.6812E+02	2.2419E+02	1.3633E+01	3.0297E+00	4.5445E+00	0.0000E+00	7.5742E+00	6.0593E+00	0.0000E+00
0.2500	1.5451E+02	1.5906E+02	1.8935E+02	1.7421E+02	1.5148E+00	0.0000E+00	0.0000E+00	1.5148E+00	6.0593E+00	7.5742E+00	0.0000E+00
0.3500	1.0755E+02	1.3785E+02	1.2270E+02	1.0452E+02	0.0000E+00	0.0000E+00	0.0000E+00	0.0000E+00	6.0593E+00	4.5445E+00	0.0000E+00

Spectra (dS/dT/dΩ) of produced particles at theta= 60.00+/- 2.00

T(GeV)	PI-MINUS	PI-PLUS	NEUTRONS	PROTONS	DEUTRONS	TRITONS	HE-3	HE-4	K+	K-	ANTIPROT
0.0500	1.3111E+02	1.1750E+02	1.2900E+03	1.1045E+03	2.9437E+02	9.2764E+01	5.3185E+01	3.6982E+02	2.4737E+00	2.4737E+00	0.0000E+00
0.1500	1.1874E+02	9.5238E+01	2.3995E+02	1.9542E+02	1.2369E+01	2.4737E+00	3.7106E+00	1.2369E+00	4.9474E+00	0.0000E+00	0.0000E+00
0.2500	1.0637E+02	9.0290E+01	1.1626E+02	1.0513E+02	2.4737E+00	1.2369E+00	0.0000E+00	0.0000E+00	2.4737E+00	2.4737E+00	0.0000E+00
0.3500	5.0711E+01	5.1948E+01	6.0606E+01	5.3185E+01	2.4737E+00	0.0000E+00	0.0000E+00	0.0000E+00	2.4737E+00	1.2369E+00	0.0000E+00

Spectra (dS/dT/dΩ) of produced particles at theta= 90.00+/- 2.00

T(GeV)	PI-MINUS	PI-PLUS	NEUTRONS	PROTONS	DEUTRONS	TRITONS	HE-3	HE-4	K+	K-	ANTIPROT
0.0500	8.7834E+01	9.7474E+01	1.1086E+03	1.0786E+03	3.1492E+02	8.4620E+01	5.2486E+01	3.2991E+02	2.1423E+00	0.0000E+00	0.0000E+00
0.1500	4.9273E+01	6.9624E+01	9.7474E+01	6.8553E+01	2.1423E+00	1.0711E+00	0.0000E+00	4.2846E+00	1.0711E+00	0.0000E+00	0.0000E+00
0.2500	2.9992E+01	2.6779E+01	2.4636E+01	1.7138E+01	0.0000E+00	0.0000E+00	0.0000E+00	0.0000E+00	0.0000E+00	0.0000E+00	0.0000E+00
0.3500	1.2854E+01	4.2846E+00	1.0711E+01	4.2846E+00	0.0000E+00	0.0000E+00	0.0000E+00	0.0000E+00	0.0000E+00	0.0000E+00	0.0000E+00

Spectra (dS/dT/dΩ) of produced particles at theta=159.00+/- 2.00

T(GeV)	PI-MINUS	PI-PLUS	NEUTRONS	PROTONS	DEUTRONS	TRITONS	HE-3	HE-4	K+	K-	ANTIPROT
0.0250	5.3801E+01	7.1735E+01	1.7814E+03	1.5363E+03	5.2008E+02	1.3151E+02	8.3691E+01	7.2333E+02	0.0000E+00	0.0000E+00	0.0000E+00

```
 0.0750 8.3691E+01 7.7713E+01 2.3912E+02 1.0760E+02 4.7823E+01 2.9889E+01 1.1956E+01 5.9779E+00 0.0000E+00 0.0000E+00 0.0000E+00
 0.1250 2.3912E+01 1.7934E+01 5.3801E+01 2.9889E+01 5.9779E+00 0.0000E+00 0.0000E+00 0.0000E+00 0.0000E+00 0.0000E+00 0.0000E+00
 0.1750 1.1956E+01 2.3912E+01 1.1956E+01 0.0000E+00 5.9779E+00 5.9779E+00 0.0000E+00 0.0000E+00 0.0000E+00 0.0000E+00 0.0000E+00

        Angle integrated spectra of produced particles
          PI-MINUS    PI-PLUS    NEUTRONS    PROTONS    DEUTRONS    TRITONS       HE-3       HE-4       K+          K-     ANTIPROT
 0.2500 2.4275E+02 2.5384E+02 9.0218E+02 8.5311E+02 1.9559E+02 4.7516E+01 3.4246E+01 2.1240E+02 9.3952E+00 4.4627E+00 1.1744E-01
 0.7500 1.1838E+02 1.3062E+02 6.4945E+01 6.0012E+01 5.1674E-01 2.3488E-02 0.0000E+00 0.0000E+00 7.2108E+00 3.3588E+00 3.9930E-01
 1.2500 7.3165E+01 8.1175E+01 3.0464E+01 2.7105E+01 2.5837E-01 0.0000E+00 0.0000E+00 0.0000E+00 6.4827E+00 2.9360E+00 2.8186E-01
 1.7500 5.3553E+01 5.8368E+01 1.7710E+01 1.7029E+01 1.4093E-01 0.0000E+00 0.0000E+00 0.0000E+00 5.0265E+00 2.2079E+00 3.0535E-01

        FISSION  CROSS  SECTIONS SIGFISP=     0.000000     SIGFIST=     0.000000
to 11:  NC=  10000 NC1=  10000 INE=  15062


EXEC TIME :  0.  3. 48. 65.

TIME PER EVENT=     0.023 SEC
```